Double-pulse Model for the Study of Red-shifted Spectrum in Multi-frequency Raman Generation

by

Zhiyu Jin

A thesis

presented to the University of Waterloo

in fulfilment of the

thesis requirement for the degree of

Master of Science

in

Physics

Waterloo, Ontario, Canada, 2023

Author's Declaration

I hereby declare that I am the sole author of this thesis. This is a true copy of the thesis, including any required final revisions, as accepted by my examiners.

I understand that my thesis may be made electronically available to the public.

Abstract

Multi-frequency Raman Generation (MRG) is a promising technique for generating few-femtosecond to sub-femtosecond pulses with high energy conversion efficiency. During transient MRG experiments coupled with two chirped pulses, when the instantaneous frequency separation between the pump and Stokes pulses is red-detuned from resonance, the individual Raman orders become a double-peak structure. These secondary peaks were only observed on the red side of the main Raman peaks.

A double pulse model (DPM) is used to describe the phenomenon of the Raman order: the Raman pulse and the red-shifted pulse. Comparison of FROG measured spectrograms with simulation using the DPM achieved lower errors compared to the Frequency Resolved Optical Gating (FROG) standard iterative program results. From the experimental results under various conditions of instantaneous frequency separations and input energies, the simulation suggested that the Raman pulse remains similar to the pump pulses, while the red-shifted pulse exhibits extra higher-order phase due to the intensity-dependent two-photon Stark shift during Raman scattering. The 4-wave mixing is more dominant in blue shifted case. DPM simulation results show that this theory of two-photon Rabi frequency shifts matches the experimental results.

Acknowledgements

Dedication

Dedicated to my parents, Xiangdong Jin and Hong Chen, who are my biggest supporter in my life. Through your sacrifices and selflessness, you have instilled in me the values of perseverance, determination, and dedication. Your belief in my abilities has given me the confidence to pursue my dreams relentlessly.

Table of Contents

List of Figures

List of Tables

List of Abbreviations

BBO   β-Barium borate (BaB_2O_4)

CCD camera Charge-Coupled Device camera

cross-FROG cross-correlation Frequency-Resolved Optical Gating

DPM   Double Pules Model

FROG   Frequency-Resolved Optical Gating

FWHM   Full Width at Half Maximum

MRG   Multi-frequency Raman Generation

SF$_6$ Sulfur Hexafluoride

SHG   Second Harmonic Generation

SPM   Self Phase Modulation

SRS   Stimulated Raman Scattering

List of Units

ps   picosecond (10^{-12} s)

fs   femtosecond (10^{-15} s)

as   attosecond (10^{-18} s)

THz   terahertz (10^{12} Hz)

μm   micrometer (10^{-6} m)

nm   nanometer (10^{-9} m)

mJ   millijoule (10^{-3} J)

List of Symbols

ϵ_0 Vacuum permittivity

ϵ Relative permittivity

λ Wavelength

ω Angular frequency

ω_0 Center-frequency

ω_R Raman frequency

χ Susceptibility

$\chi^{(2)}$ Second order nonlinear susceptibility

$\chi^{(3)}$ Third order nonlinear susceptibility

$\chi^{(n)}$ n-th order nonlinear susceptibility

Ω Rabi frequency

Ω' Generalized Rabi frequency

c Speed of light

Δ Detuning

Chapter 1

Introduction

1.1 Multi-frequency Raman Generation

In recent years, more and more attention than ever before has been paid to how to create ultrafast pulses with high intensity. Multi-frequency Raman generation (MRG) is one of the most efficient techniques to produce ultrafast pulses with a wide discrete spectrum by nonlinear optical process [1]. The process of generating attosecond pulses using high harmonic generation has been invented for many years but the efficiency is not high. However, MRG could make single femtosecond ultrafast pulses with enough intensity to observe the dynamic reactions of molecules [2].

In MRG experiments, the individual Raman orders became double peaked when the researchers tuned the instantaneous frequency separation of the two pumps to the red side of the Raman transition [3]. The red shifted spectrum can be observed from the measurement results of the Frequency Resolved Optical Gating (FROG) [4].

The MRG refers to multiple orders of anti-Stokes and Stokes generated when two strong pulses drive the Raman Scattering. The process is shown in Figure 1.1 below.
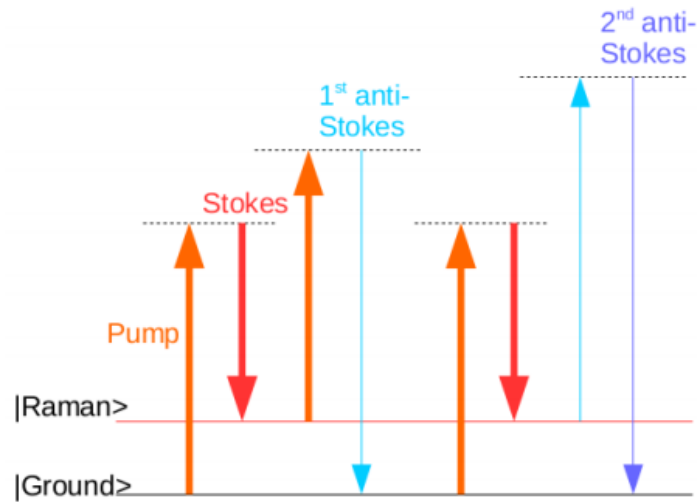
Figure 1.1. Energy level diagram of MRG with the generations of 1st and 2nd anti-Stokes Raman orders [5].

The pump beam activates the molecules to a virtual energy level from the ground energy level. The molecular energy will be noted to come down, but due to the coupling by the Stokes, it will not come down to the ground energy level but to the Raman energy level. The pump beam can again pump these molecules in the Raman level to a new virtual energy level, and after this, a new photon with a higher frequency will be released as the molecule drops to the ground energy level, and this is referred to as the Raman first order anti-Stokes.

These first anti-Stokes photons act as new pump beams upon accumulation and will readily take the molecule to the higher virtual energy level. The second anti-Stokes Raman order will thus be created when the molecule returns to the ground energy level [6]. This process will result in a wide discrete spectrum as it continues and cascades. The Raman frequency of the material separates the orders of a wide discrete spectrum resulting from this process. Studies have shown that each Raman order generated as a cascaded simulated Raman scattering (SRS) is of the third order nonlinear process, the $\chi^{(3)}$ ($\omega_j+\omega_R$; ω_j, $\omega_j-\omega_R$, ω_j). The jth of the anti-Stokes order is

represented as ω_j [7].

Research shows a close relationship between MRG and Raman scattering in that as Raman scattering occurs in solid, liquid and gas Raman materials, so does MRG. The most widely used Raman medium is gas, which are small dispersion materials [8]. The adiabatic, impulsive, and transient are the three regimes that MRG works depending on the pump pulse duration. An impulsive regime is noted when the pulse duration decreases continuously and becomes less than the period of vibration. For the transient regime, the pulse duration and dephasing time are comparable. In the Adiabatic regime, the dephasing time is less than the pulse duration of the molecules [2].

1.2 Experiment of Multi-frequency Raman Generation

Previously, our group conducted MRG experiment in the transient regime [9], where sulfur hexafluoride (SF6) was used to generate various Raman orders. The main reason for using SF6 is its compatibility with the laser setup in the lab, as its Raman frequency matches the laser spectrum. The lab employed a dual wavelength Ti:Sapphire laser system [10] to generate two pump pulses with spectra centered at 786 nm and 837 nm. The frequency separation between these two pump beams is precisely chosen as 23.25 THz to align with the vibrational Raman frequency of Sulphur Hexafluoride (SF6). Each of the two pulses, possessing a spectral bandwidth of approximately 3 nm, are independently directed to the triple-grating compressor for compression. The temporal spacing between the pulses of the two pump beams can be modified by displacing the back mirror, M7.
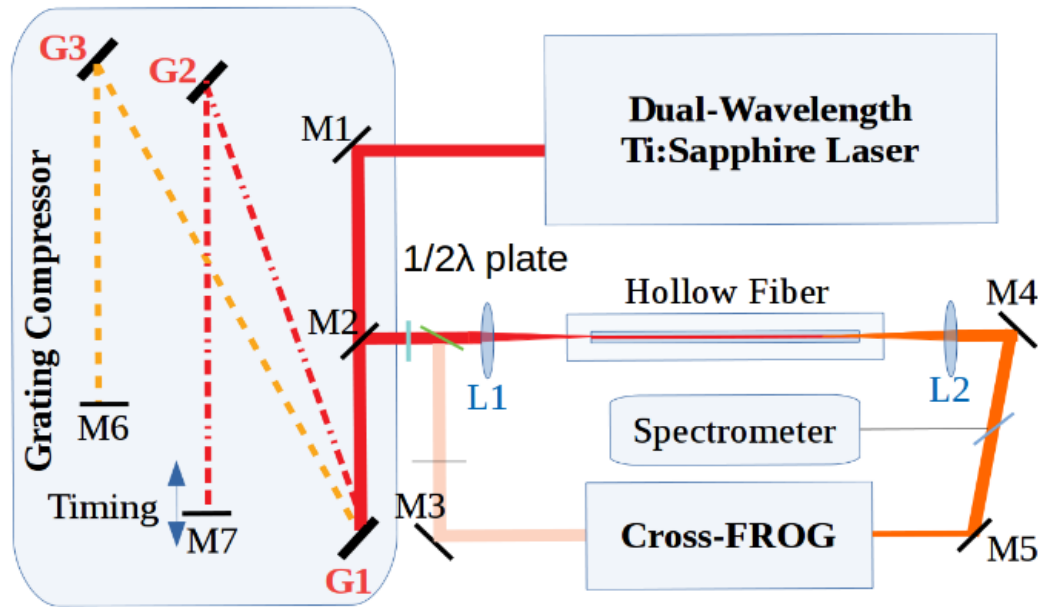
Figure 1.2. Schematic diagram of the experiment setup: M-mirror; G-grating; L-lens. [11].

To prevent self-phase modulation (SPM), a linear chirp is introduced to each pump pulse by placing a grating in an optimal position [9] [12]. One of the back mirrors in the grating compressor is adjustable, enabling control over pump pulse delay and instantaneous frequency separation. The pump pulses, carrying a total maximum energy of 2.2 mJ, are directed into a hollow fiber filled with SF6 gas. This setup generates different Raman orders, spanning from the infrared to the ultraviolet range, exhibiting a strong correlation with the pump pulses in terms of chirp characteristics.

The two pump pulses were subjected to second harmonic FROG measurements to verify their similar chirps [4]. The FROG reconstruction revealed that the pump pulse had a duration of 900fs FWHM, with a chirp rate of 1.6THz/ps. Meanwhile, the Stokes pulse had a duration of 830fs FWHM and a chirp rate of 1.5THz/ps. To reduce uncertainties in the spectrogram of the first anti-Stokes order with double peaks, a cross-FROG measurement was performed using the Stokes pulse as one of the input

pulses.

Two sets of measurements were conducted to analyze the electric field of the first anti-Stokes order [7]. In the first set, the time delay between the two pump pulses was set at 333fs, with the higher frequency pump pulse preceding the lower frequency Stokes pulse. This delay resulted in a red shift of the instantaneous frequency separation by approximately 0.5THz. At this red shift, the maximum number of Raman orders and the maximum red shift of the second peak in each order were observed. The average energy was varied from 2.2mJ to 1.7mJ to 1.2mJ. In the second set of measurements, the energy was fixed at the maximum level of 2.2mJ, and the time delay was adjusted to increase the red detuning from 0 to +666fs in increments of 333fs [7].
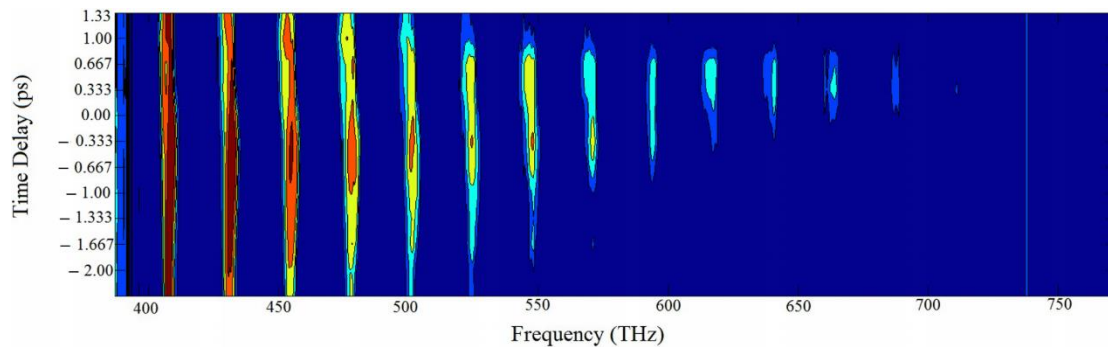
Figure 1.3. The multi-frequency Raman generation (MRG) spectra are shown for two positively chirped pump pulses with total energy of 2 mJ as a function of time delay between the two pulses [16].

In Figure 1.3, the MRG spectrum from the spectrometer as a function of time delay is shown and there is a spectrum peak on the red side of each main Raman peak. This could result from the SPM, but it is eliminated by the grating in the experiment set. It is also not from the 4-wave mixing effect because the extra peak would move on a

5

diagonal line with time delay if the 4-wave mixing exist, but there are only two lines in the MRG spectrum. Hence, it should from other effects such as Rabi frequency and Stark shift.

In conclusion, the MRG experiment involves several processes, including seeding, amplification, compression, and spectral measurements. Red-shifting phenomenon and the generation of anti-Stokes Raman orders are observed. The FROG setup is used for pulse measurements, and spectrometer measurements provide information about the generated spectrum. In MRG experiments, the phenomenon of individual Raman orders exhibits a double-peaked structure is observed when the instantaneous frequency separation between the pump and Stokes pulses is red-detuned from resonance. The secondary peaks are generated only on the red side of the Raman peaks. Other research groups also observed this occurrence [12][13][14]. The red-shifted spectrum has the potential to produce higher-power pulses, making it an area of interest for further investigation. Further studies are needed to explore the red-shifted spectrum and its impact on ultra-short pulse generation.

1.3 Frequency Resolved Optical Gating

Frequency Resolved Optical Gating is a main pulse measurement tool [4]. It can record the two-dimensional trace of the retrieved electric field in time domain and frequency domain [7]. FROG has become a wide-spread technique for ultra-short pulse measurement, which can be applied to a wide range of wavelengths.

There are various variants of FROG, and they have different advantages and disadvantages in different circumstances. Due to the much higher sensitivity, Second Harmonic Generation (SHG) FROG becomes the most widely used FROG. It mainly

uses the nonlinear effect of the nonlinear crystals χ (2) to process the two input ultra-short pulses, and finally produces a signal with twice the frequency. There is an ambiguity of the direction of time, but it can be removed with extra information.
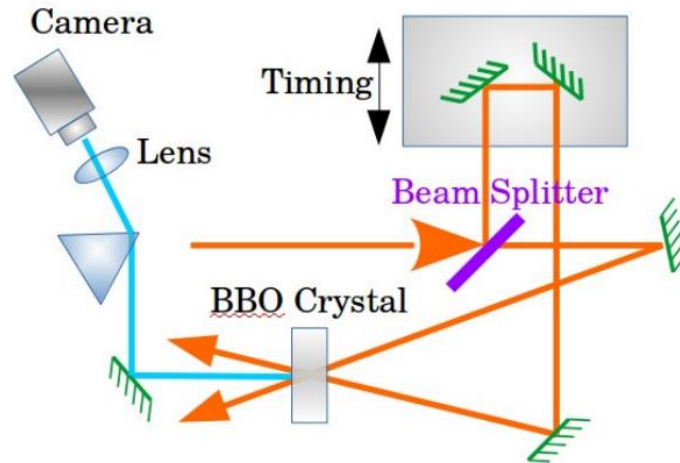
Figure 1.4. The Schematic of auto-correlator with BBO crystal. BBO: β-Barium borate (BaB_2O_4) crystal. CCD camera: Charge-Coupled Device camera [7].

In our experiment, the single-shot FROG is used to achieve the time delay between the pulses [7]. In an auto-correlator setup, the pulse beam is split into two pulses with different time delay. These two pulses are sent into the BBO crystal, a nonlinear material, with a special angle.
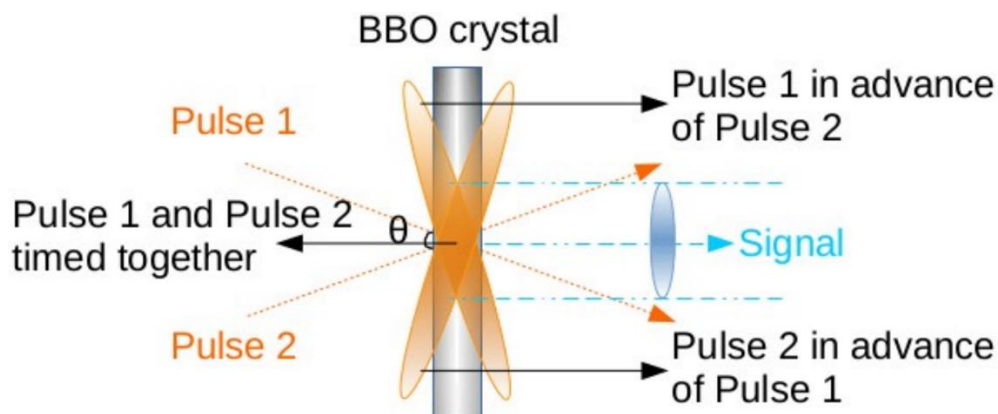
Figure 1.5. Two pulses correlating in a single-shot FROG with time-delay achieved by crossing two thin lines at an angle θ [7].

The two pulses are focused by a cylindrical lens in the vertical direction, but the pulses stay the same in horizontal direction. As shown in Figure 1.5, to make sure the two pulses overlap each other within the BBO crystal as a horizontal thin line, the BBO crystal is positioned at the focal point of the cylindrical lens.

The correlation of the two pulses happens in the BBO crystal and the two pulses are timed together in the center. The front of pulse 1 and the back of pulse 2 overlap with each other at the upper side while the back of pulse 1 and the front of pulse 2 overlap with each other at lower side.
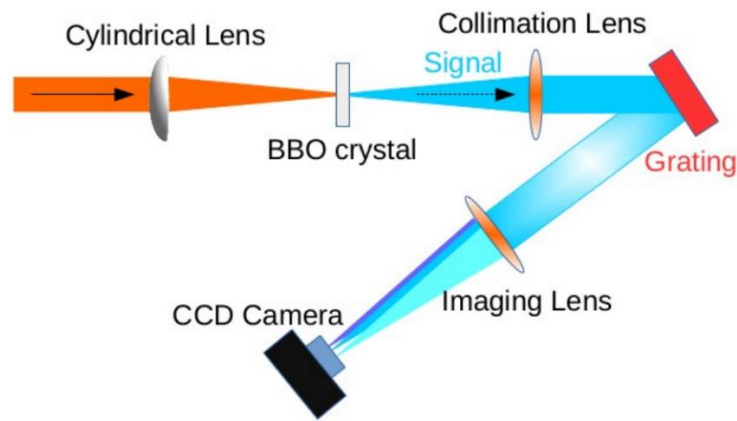
Figure 1.6. Single-shot FROG recording system (side view) [7].

From Figure 1.6, after the signal goes through the collimation lens, the grating disperses the signal. the time delay information from the correlation is in horizontal direction of the signal and the spectral information from the correlation is in vertical direction of the signal [7].

The signal is collected by the CCD camera and the intensity can be measured by Equation (1).

$$I_{sig}^{SHG}(\tau) = \int_{-\infty}^{\infty} I(t) I(t-\tau) dt$$

(1) [7]

8

In Equation (1), τ is the time delay between the two pulses. After processing the data, it is impossible to solve one-dimensional phase retrieval problems, so it is transformed into two-dimensional phase retrieval problems, which can be solved under some circumstance.

For FROG Algorithm, the iterative Fourier Transform Algorithm is used, and the specific process is shown in Figure 1.7.
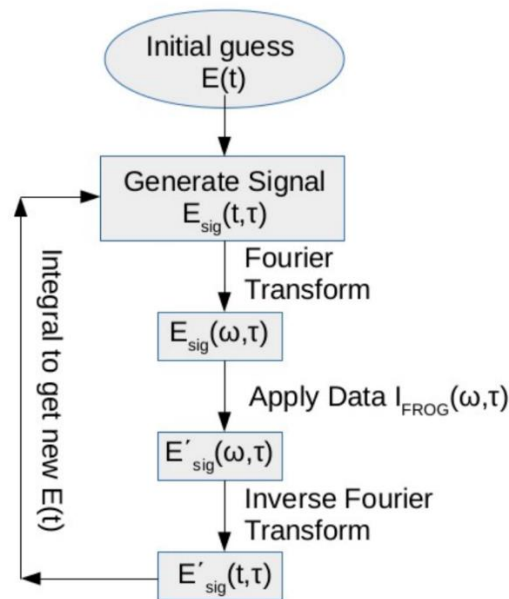
Figure 1.7. Iterative Fourier Transform Algorithm [7]

Professor Rick Trebino's team created a program to do the simulation and it can retrieve amplitude and phase of the field from its FROG trace. It is a very effective program to achieve pulses, but it is difficult to find out what the two input ultra-short pulse are. Dr. Zujun Xu and Professor Donna Strickland developed a new algorithm and program to gain the double pulse model simulation trace and the chirp of the two input pulses [5].

The electric field of the broadened first anti-Stokes Raman order is retrieved by the standard second harmonic FROG [15]. However, the reconstructed electric field from

second harmonic FROG is too complicated to provide a unique result. This complicated structure is on account of the broadened order is a result of two pulses overlapping both spectrally and temporally. Therefore, a new way to do the double pulse model simulation needs to be discovered. In this stage, a Python program is used to simulate the FROG trace again to obtain the input of two ultra-short pulses.

The researchers assume that the main differences between them are their center frequency, time delay, amplitude, and phases. Therefore, the idea is to set two pulses, E_1 and E_2 in Python. The program overlaps E_1 and E_2 to produce a double pulse model simulation trace. After that, the program will compare the double pulse model simulation trace and the original FROG trace and the error between them will be obtained. In the next stage, several parameters of E_1 and E_2 are changed, such as center frequency, time delay, amplitude, and extra phases, to reduce the error between them. When the double pulse model simulation trace obtained by this method is very close to the experimental FROG spectrogram results, the error becomes small enough and the iteration stops. After that, the simulated E_1 and E_2 can be regarded as the two input ultra-short pulses that generate the original trace in the experiment. This project is to create a new algorithm that can do the double pulse model simulation and obtain the chirp of the two input ultra-short pulses in the FROG experiment. I used this double pulse model simulation to reveal that the red-shifted spectrum is caused by a two-photon dressed-state Rabi frequency and Stark shift [16].

Chapter 2

Double Pulse Model Simulation

2.1 Concept of Double Pulse Model Simulation

In this chapter, the red shifting phenomenon with double pulse model for the anti-Stokes pulse will be explained. The anti-Stokes pulse is formed by two pulses: the Raman pulse and another pulse with an extra phase added to it, called red shifted pulse.

(a) 0 fs   (b) 333 fs   (c) 666 fs
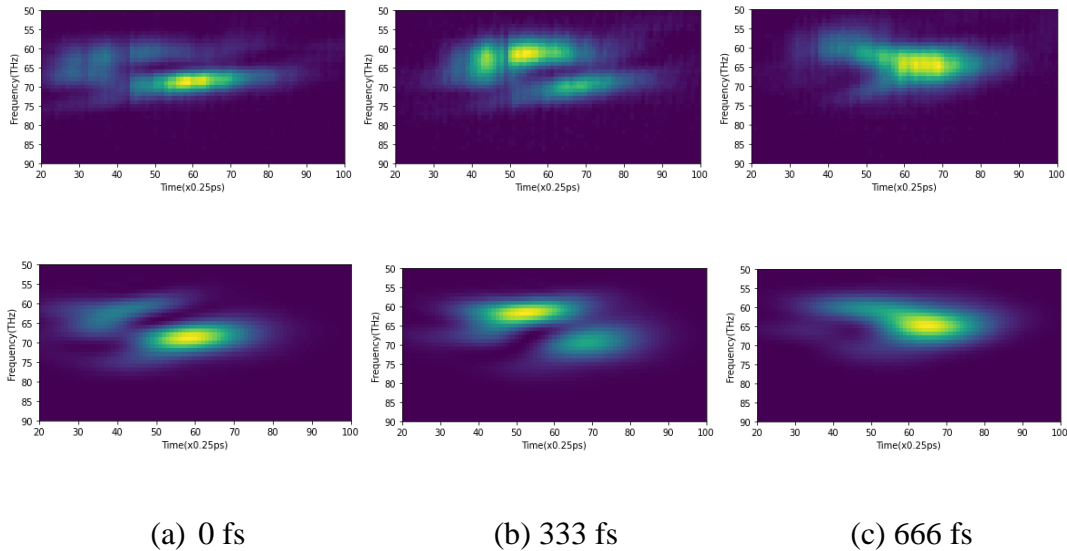
Figure 2.1. Example of experimental trace and DPM simulation trace. Top: The original experiment traces. Bottom: DPM simulation traces. The time delays are at 0 fs, 333 fs, and 666 fs from left to right [5].

In Figure 2.1, the program compares the simulated trace with the original trace. With the help of the FROG, reasonable simulation results are obtained, but the information for phase, chirp rate and other properties of total Raman pulse and red shifted pulse is missing. Therefore, the double pulse model was designed by Zujun Xu and me in the

hope that it can help researchers gain a better understanding of Raman pulse and red shifted pulse. I wrote my own code and that I concentrated on studying the time delay results with my program.

In the beginning, the gaussian shape pulse is used to define the Raman pulse (E_1) and red shifted pulse (E_2) in the program. The total Raman pulse (E) is equal to Raman pulse plus red shifted pulse.

$$E(t) = E_1(T_1, \omega_1, \phi_1, t) + \alpha E_2(T_2, \omega_1, \phi_2, t) \ (2) \ [7]$$

In the double pulse model simulation, the time duration (T_1 and T_2), center frequency (ω_1 and ω_2), the intensity ratio (α), the phase (ϕ_1 and ϕ_2), and the time delay (t) of the two gaussian pulses, E_1 and E_2 are adjustable.

$$\text{Phase} = \int (\text{Instantaneous Frequency}) * dt \ (3)$$

The most important and controversial parameter is the phase. The instantaneous frequency, also called time dependent frequency, is used to decide what the phase is for the pulses. The integral of the instantaneous frequency is equal to the phase of the pulse. For the Raman pulse, the time dependent frequency should be a linear chirp. For the red shifted shoulder pulse, I believed that there was not only a linear chirp, but also a second order chirp. From Equation (3), The integral of the instantaneous frequency is the second order phase for both the Raman pulse and the red shifted pulse, and the third order phase for red shifted pulse.
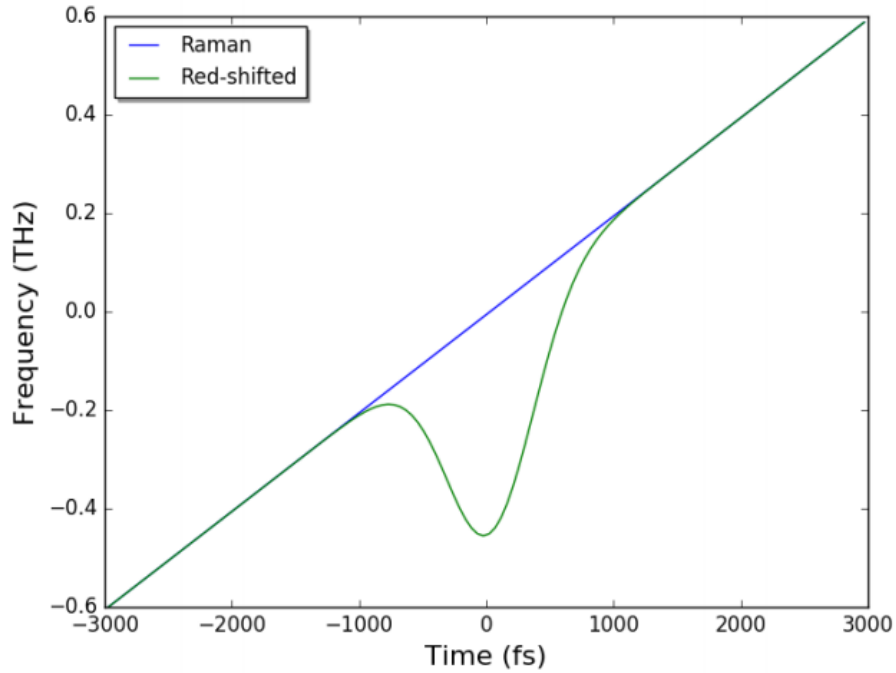
Figure 2.2. Instantaneous frequency of Raman pulse and red-shifted pulse.

After studying the simulation results, another idea about the phase of the red shifted shoulder was provided. The instantaneous frequency of red shifted shoulder consists of the linear chirp and a gaussian shaped dip chirp in the middle instead of a second order chirp [5].

2.2 Stark Shift and Rabi Frequency

As a group of parallel monochromatic plane waves, Lehmberg et al. treated the Raman orders as the waves travelling through the Raman medium together, which was dispersion less [17]. A discrepancy was noted between the conversion rate calculated, and that observed from the experiment [18]. The experimental conversion rate was more ordered than the calculated conversion, which was ordered less. The theory of Lehmberg et al. was then generalized by Hickman et al., who fully

13

considered molecular excitation. A set of frequency components ($\omega_j = \omega_0 + j\omega_R$) were used to depict the propagation of the process and the two-photon Bloch equation employed in describing the interaction of the field. The coupled equation for the electric field obtained is given as [19].

$$\frac{\partial E_j}{\partial z} = \frac{\omega_j}{2\omega_R} \frac{\partial \Omega}{\partial z} \sqrt{(\Omega^2 + B^2)}\left(E_{j-1} - E_{j+1}\right) \quad (4)$$

The Rabi frequency here is denoted as Ω, while the initial condition as B. Ω (Rabi frequency) is given by the expression below:

$$\Omega e^{i\theta} = \frac{\alpha_{12}}{2\hbar} \sum_j V_j V_{j-1}^* \quad (5)$$

$$\Omega'^2 = \Omega^2 + \Delta^2 \quad (6)$$

$$\Delta = \frac{\partial \theta}{\partial t} + \frac{2\pi(\alpha_{22} - \alpha_{11})I}{\hbar c} + \delta\omega \quad (7)$$

When detuning, Rabi frequency and intensity are generalized, they are given as [19]

$$I = \frac{c}{8\pi} \sum_j V_j V_j^* \quad (8)$$

The jth Raman order amplitude is the V_j, and the transition moment is denoted as α_{ij}. Between the Raman frequency and the pump's frequency separation, the detuning present is denoted as $\delta\omega$. As shown in the Equation (5), there is a relationship between adjacent amplitudes generated and the Rabi frequency [20]. Equation (7) shows a relationship between the beam's total intensity, including anti-Stokes, Stokes, and pulses of the pump, and the intensity I. It is evident from Equation (7) that the intensity, I, Raman frequency detuning $\delta\omega$, and the overall rate of change of phase θ, are the three terms that are employed in the determination of the detuning Δ.

14
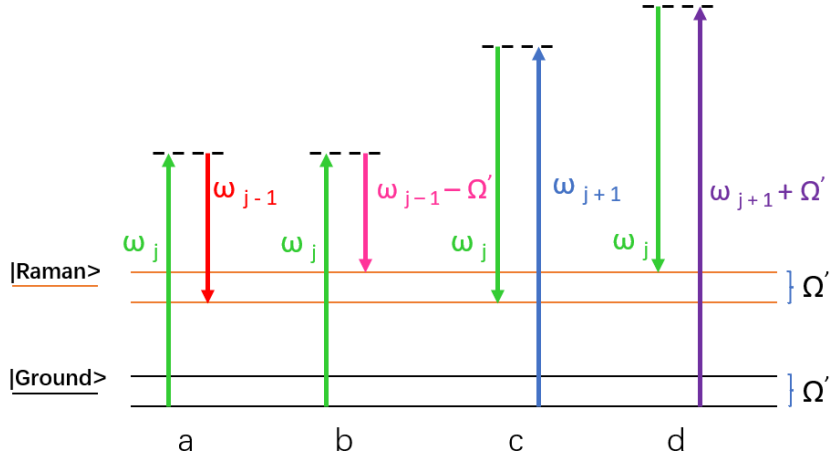
Figure 2.3. Linear Raman scattering diagram of two-photon dressed states. ω_{j-1}, ω_j, and $\omega_{j+1}$are center-frequencies of Raman orders, Ω' is the generalized Rabi frequency [5].

In many MRG experiments, the red shifted shoulder is observed in the wide spectrum. The two-photon dressed states are used to explain it as shown in Figure 2.3. Each of the energy levels will split into two coherent states with a frequency separation of Ω'. In Figure 2.3, the lower level is predominantly populated. The process (a) is emission of the Raman photons. The process (b) emitting a red-shifted photon; and. The process (c) is absorption of the Raman photons and process (d) is absorption of a blue-shifted photon. With the linear Raman scattering, each of the Raman orders will only show red-shifted shoulder.

In the Equation (5), (6), (7) and (8), the Ω' is the generalized Rabi frequency, the Ω is the Rabi frequency, the Δ is the detuning, and I is the total intensity of the beam. From Rickes' paper [21], the Hamiltonian is used to illustrate the two-photon two-state process.

15

$$H(t) = \hbar \begin{bmatrix} D_1(t) & \Omega(t)/2 \\ \Omega(t)/2 & D_2(t) \end{bmatrix} \quad (9)$$

$$D_1(t) = S_1(t) \quad (10)$$

$$D_2(t) = S_2(t) + \Delta_0 \quad (11)$$

The $\Omega(t)$ is the Rabi frequency and D_1 and D_2 are the diagonal elements of this Hamiltonian include dynamic Stark shifts $S_1(t)$ and $S_2(t)$ for the two states, which can be considered as a part of detuning. The Δ_0 is the constant detuning and S(t) is the Stark shift. In addition, the Equation (5), (6), (7) and (8) can be written as in the form below.

$$E^{\pm}(t) = \frac{\hbar}{2}[\Delta(t) \pm \sqrt{\Omega^2(t) + \Delta^2(t)}] \quad (12)$$

$$|E^+(t) - E^-(t)| = \hbar\sqrt{\Omega^2(t) + \Delta^2(t)} \quad (13)$$

$$\Delta(t) \equiv D_2(t) - D_1(t) = \Delta_0 - S(t) \quad (14)$$

Where the E^+ and E^- are the adiabatic energies and the square of $|E^+(t) - E^-(t)|$ is the generalized Rabi frequency. The $\Omega(t)$ is the Rabi frequency and the $\Delta(t)$ is the total detuning.
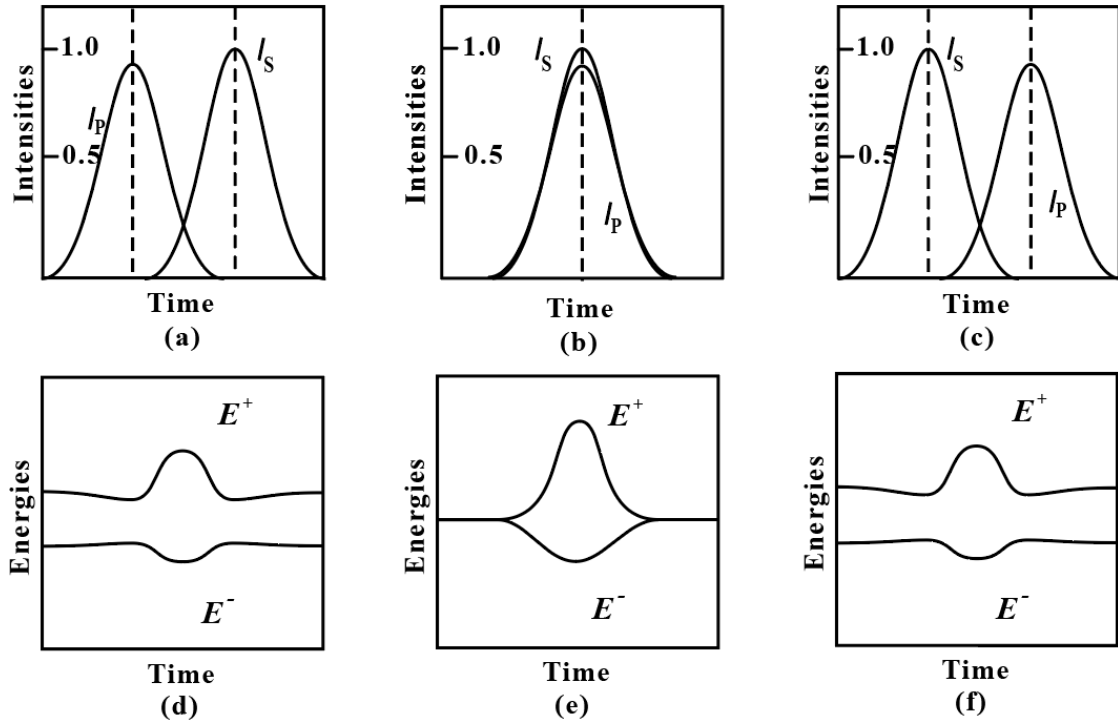
Figure 2.4. Energy levels resulting from the two-photon Bloch equations. (a), (b) and (c) show the relative timing and pulse durations of the two pump pulses. (d), (e) and (f) show the energy levels resulting from the two-photon Bloch equations for the corresponding time delays shown above each figure.

The adiabatic passage from ground state to intermediate state occurs at the first resonance. However, the population returns to the initial state by adiabatic passage at the second resonance. From Equation (13), the general Rabi frequency is equal to the square of $|E^+(t) - E^-(t)|$. From experimental results, there are only the red shifted shoulders and blue shifted shoulders that do not exist. As shown in Figure 2.4, during the Raman scattering, the Raman states split into states E^+ and E^-. When the Raman photons are absorbed by the intermediate state, they can reach both the E^+ and E^- states. On the contrary, when the photons are emitted from the intermediate state to Raman state, they can only reach the E^+ state. Hence, only red shifted pulse and the pump pulse are obtained.
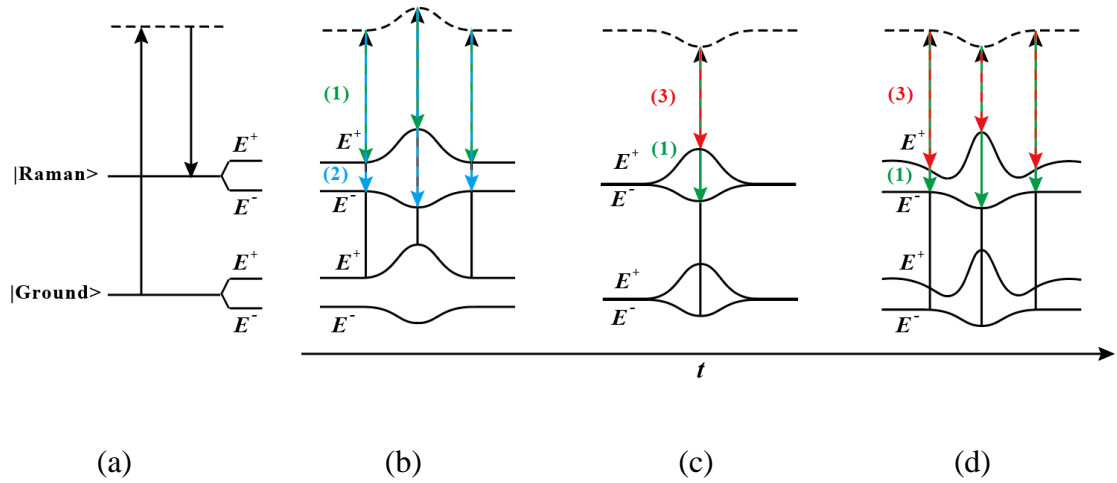
Figure 2.5. Energy levels in states. (a) Linear Raman scattering diagram with split states E^+ and E^-. (b) The adiabatic energies (E^+ and E^-) for blue shifted pulses. (c) The adiabatic energies for timed pulses. (d) The adiabatic energies for red shifted pulses. The process of black arrow line is the absorption of pump pulse. The process (1) emits Raman pulses. The process (2) emits blue shifted pulses. The process (3) emits red shifted pulses.

In order to explain the red shifted shoulder in MRG, the theory of Rabi frequency and Stark shift are introduced into double pulse model simulation. From this theory, the Raman level and ground level can be split into two sub-levels by two-photon Stark shift in the Raman process. The frequency separation must be red shifted to remain in resonance to efficiently generate several anti-Stokes orders. With the red shift, the lower level is predominantly populated, it is clear from Figure 2.5 that there are three possible linear Raman transitions. For process (a), it is the emission and absorption of Raman photons. In process (b), the photons start from the E^+ level of ground state and they pump up to the E^+ level of intermediate state. In the end, some of the photons come back to the E^+ level of Raman state, which is the Raman pulse, while others emit to the E^- level of Raman state so this process also generates blue shifted pulse. The process (c) is emitting a red-shifted photon for resonant case. The photons start

18

from the E⁻ level of ground state and they pump up to the E⁻ level of intermediate state. In the end, some of the photons come back to the E⁻ level of Raman state, which is the Raman pulse, while others emit to the E⁺ level of Raman state so this process also generates red shifted pulse. Process (d) is also the Raman and red shifted photons emission.

From Equation (6), the generalized Rabi frequency can be written in a function of Rabi frequency, the laser detuning, and the Stark shifts. From the Equation (7), the Stark shift is pulse intensity dependent. Hence, the generalized Rabi frequency is pulse intensity dependent. It provides the frequency separation of the instantaneous frequency between the Raman and shifted pulses.

Therefore, the generalized Rabi frequency can be drawn as shown in Figure 2.6 in the program.
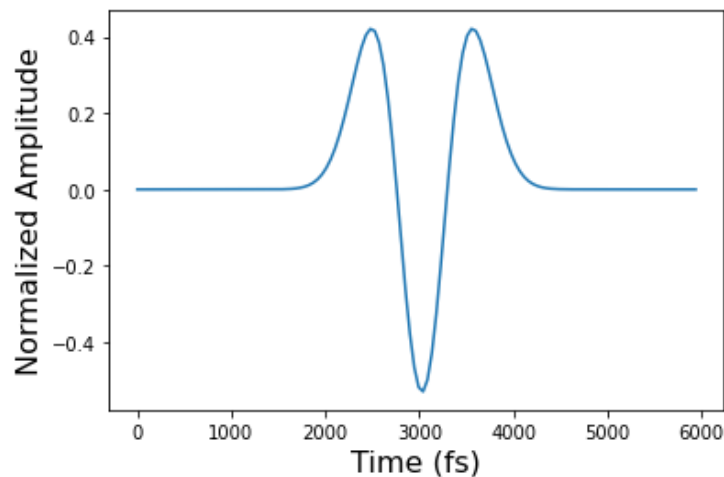
Figure 2.6. Generalized Rabi frequency.

From the view of the instantaneous frequency, the generalized Rabi frequency is added to the instantaneous frequency of the red shift pulse as shown in Figure 2.7. It will look like a linear chirp added a gaussian dip and two gaussian humps on the side

of it. The separation between the chirp is from the constant detuning Δ_0.
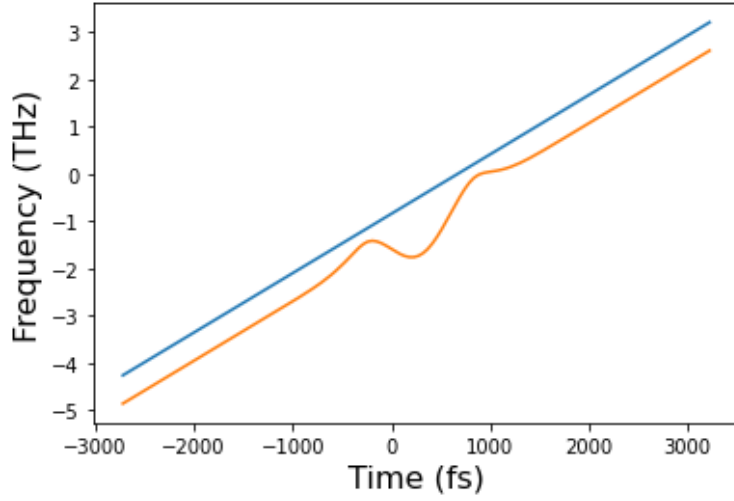
Figure 2.7. Instantaneous frequency with theorical generalized Rabi frequency. The blue linear chirp is the instantaneous frequency of the Raman pulse. The red chirp is the instantaneous frequency of the red shift pulse.

As for the amplitude ratio between Stark shift and Rabi frequency, it depends on the coefficients, α_{12}, α_{11} and α_{22} in Equation (5) and (6). In the experiment, the Sulphur Hexafluoride (SF_6) is used in the Hollow Fiber to resonate and the number of α_{12}, α_{11} and α_{22} are at around $1.65456e\text{-}31\ m^3$, $1.64378e\text{-}31\ m^3$ and $1.66841e\text{-}31\ m^3$ respectively. From the above equations and α_{12}, α_{11} and α_{22}, the amplitude ratio between Stark shift and Rabi frequency is equal to 1: 60 approximately. Hence, the gaussian dip in the middle is much more dominant than the two gaussian humps on the side so the instantaneous frequency of the red shift pulse is consisting of a linear chirp and a gaussian shape dip in the middle in Figure 2.8.
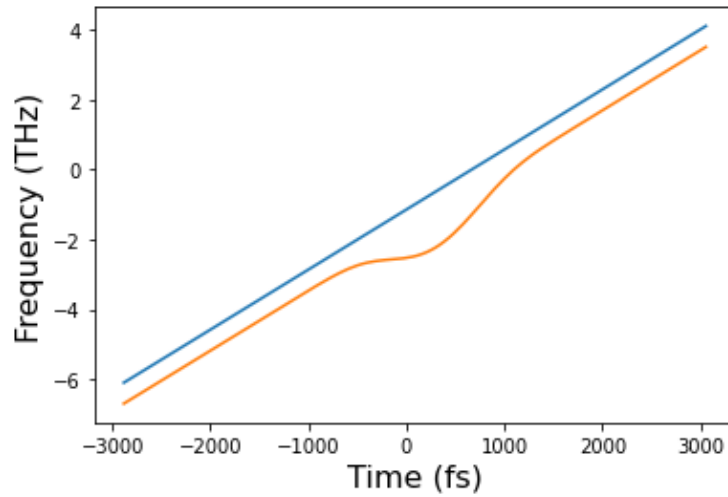
Figure 2.8. Instantaneous frequency with actual generalized Rabi frequency. The blue linear chirp is the instantaneous frequency of the Raman pulse. The red chirp is the instantaneous frequency of the red shift pulse.

2.3 Component of Simulated Pulse

From Equations (2) to (13), the phase and instantaneous frequency of Raman pulse (E_1) and red shifted pulse (E_2) can be defined in Python program to do the double pulse model simulation. The code is shown below.

```
def FROGs(T1,T2,A,f0,a,a2,ph0,ff,TT0,tt,tpp):

    f1 = gaussian_pulse(TT0,0,1.0,0,tt)   #generate Gaussian pulse E-field

    f2 = gaussian_pulse(TT0,0,1.0,0,tt+tpp*dd)

    i1 = f1**2

    i2 = f2**2
```

21

```
i3 = i1*i2

i3 = np.sqrt(i3)

i4 = i1 + i2

Stark = -2*np.pi*(a22-
a11)*A0*ff*i4/(c0*h/(2*np.pi))/(10**12)+tpp/1000*i_t/1000

Omega = 2*np.pi*a12*A0*ff*i3/(c0*h/(2*np.pi))/(10**12)

e_diff = np.sqrt(Stark**2+Omega**2)


phase1 = a2*(t-tt)#+a3*(t-tt)**2                    #zero phase at pulse peak

phase1 = integral(-phase1)

phase1 = phase1-phase1[63]


phase2 = a2*(t-tt)-e_diff*2*np.pi#+a3*(t-tt)**2

phase2 = integral(-phase2)

phase2 = phase2-phase2[63]+ph0


E1 = gaussian_pulse(T1,f0,A,phase1,tt)        #generate Gaussian pulse E-field

E2 = gaussian_pulse(T2,f0,1.0,phase2,tt)

E = E1+E2
```

```
FROG = FROG_generator(e,E,TD)

delta_d = array_diff(FROG, original_trace)

return FROG, delta_d
```

In the program, there are 10 different parameters to control the simulation of the total Raman pulse. They are T1 (Pulse duration of the Raman pulse (E_1)), T2 (Pulse duration of the red shifted pulse (E_2)), TT0 (Pulse duration of generalized Rabi frequency), f0 (Center frequency), tt (Time delay), tpp (Time jitter), a2 (The chirp rate of instantaneous frequency), ph0 (Π phase shift) and ff (Amplitude coefficient of Rabi frequency). The i_t is the parameter, which controls the frequency separation of the instantaneous frequency of E_1 and E_2 for different cases.

The Stark shift is the total detuning, $\Delta(t)$. The Omega is the Rabi frequency, Ω. The e_diff is the total Rabi frequency, which is shown in Equation (13). The phase of Raman part is only a second order phase, which is the integral of a linear instantaneous frequency. Meanwhile, the phase of the red shifted part consists of a second order phase, a pi phase shift and the integral of generalized Rabi frequency. The E_1 and E_2 are Raman pulse and red shifted pulse. E is the total Raman pulse.

2.4 Iteration Method

The code contains several parts. The first part is used to create a system that compares the difference between the original trace from the experiments and the simulated trace. It can provide the errors that tell us if the simulated trace is a good match. Secondly, the total Raman pulse and its initial condition and the limitation of the parameters are

23

defined. After that, the program will start an iteration process. It will begin to change the value of one of the parameters in the limitation set by the operators. The error of the simulation with different value of the parameter are compared. For instance, the time duration of the Raman part pulse T1 is limited to between 800 fs and 1000 fs, and the code will first calculate the error with T1 at 800 fs, 801 fs, 802 fs until 1000 fs. When it reaches 1000 fs, the calculation will stop and start to compare the errors. The lowest error among them will be selected and use its value of T1 to do the simulation of the next parameter. After all the parameters have been processed, the program will do the same simulation again, again and again until an acceptable error appears.

Chapter 3

Results Analysis

3.1 Simulation Data of Double Pulse Model
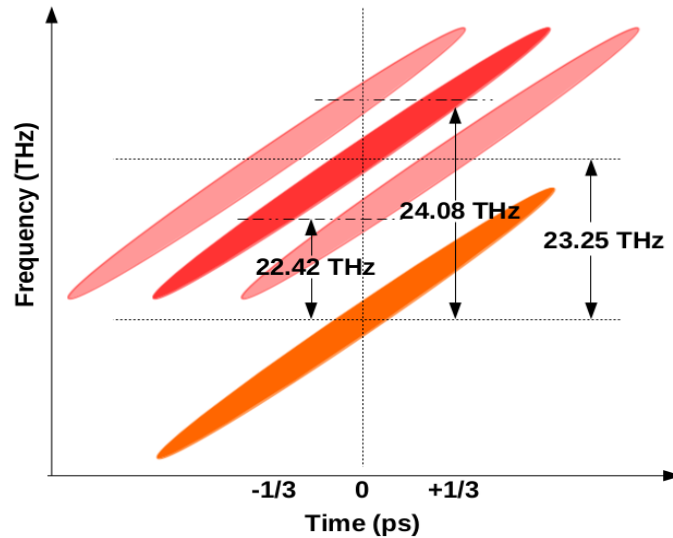
Figure 3.1. Instantaneous frequency separations with different time delays between the pump(red) and the Stokes(orange)

For the experiment results, there are five data sets with different time delays. Each of the data sets have 11 original traces. They are labeled as five data sets, A (23.75THz), B (23.25THz), C (22.75THz), D (22.25THz) and E (21.75THz) cases. The case A is the most blue shifted one, the case E is the most red shifted one. The case C is the overlapped one. From the theory, the constant detuning in the instantaneous frequency should be almost 0 for the case C. The constant detuning for the case B and D should be around 330 fs in time domain. The constant detuning for case A and E should be around 660 fs in time domain. If all five data sets provide good matches with the above condition, then the simulation matches the theory.

25

Data Set	Raman pulse simulation trace	Blue shifted pulse simulation trace	Double pulse model simulation trace	Original trace
1				
2				
3				
4				
5				
6				

7			
8			
9			
10			
11			
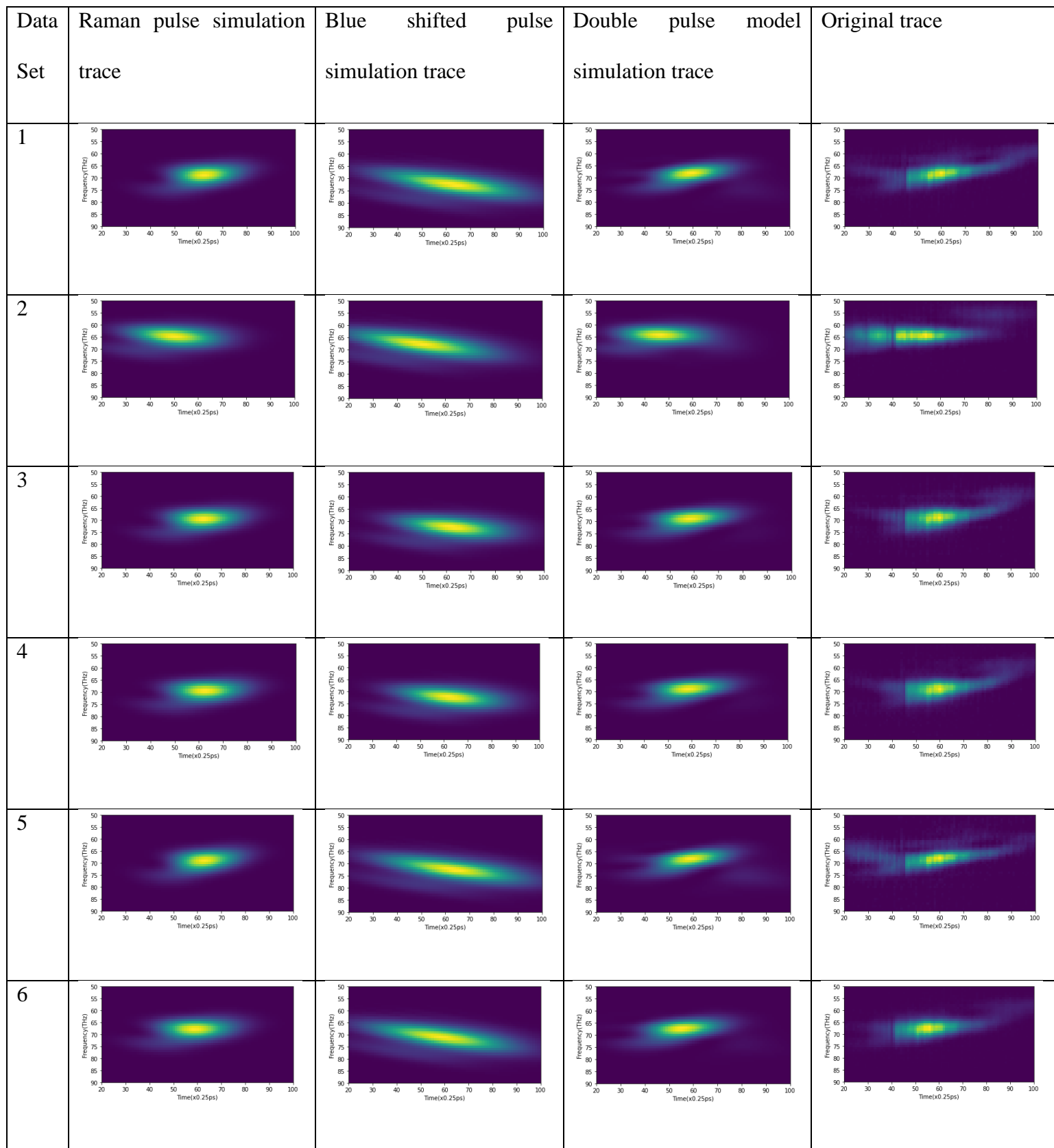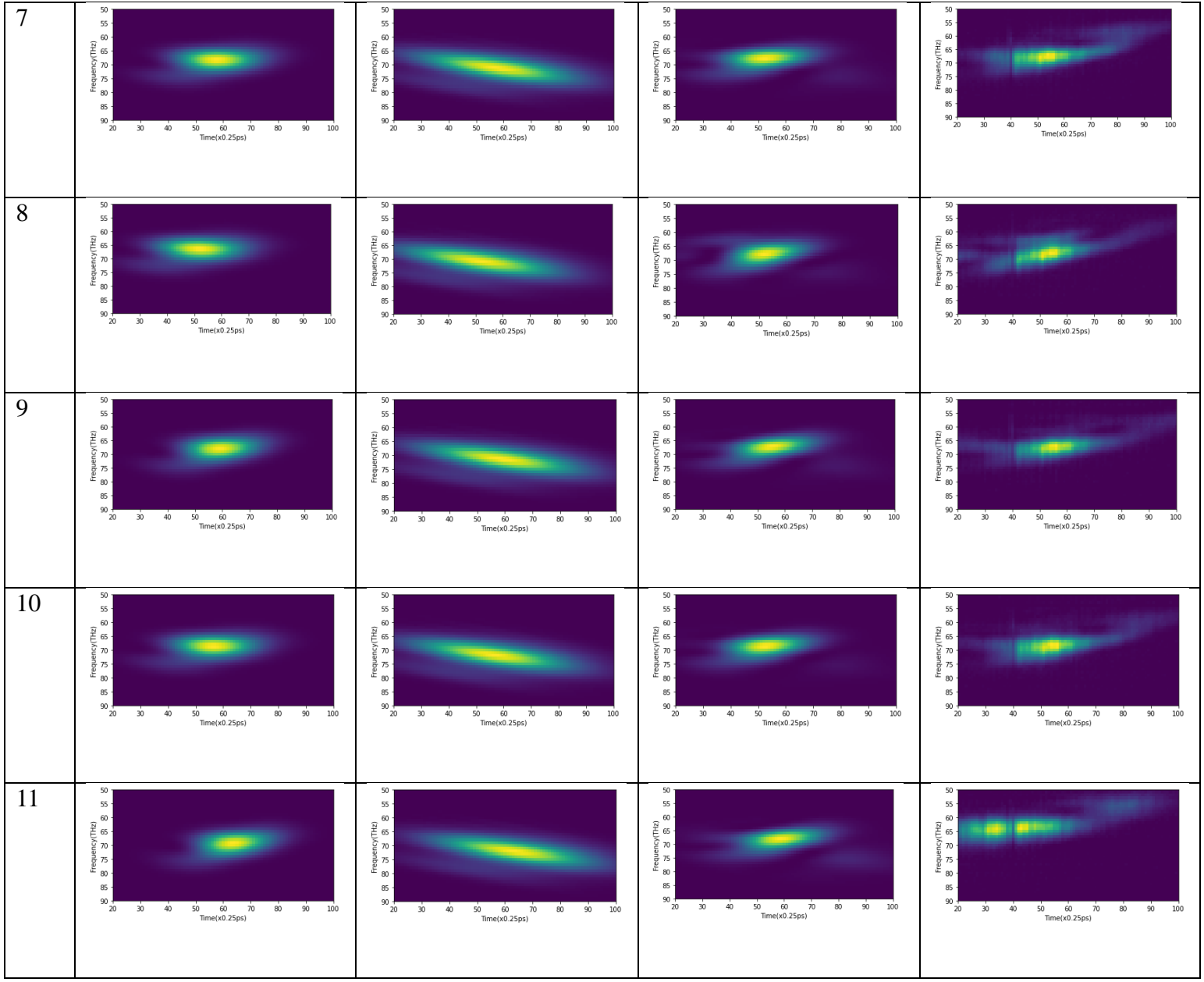
Table 3.1. Simulated and original trace for 11 data set of case A. Unit for x-axis: 46.77109 fs/pixel. Unit for y-axis: 0.1670369 THz/pixel.

27

Data Set	Raman pulse simulation trace	Blue shifted pulse simulation trace	Double pulse model simulation trace	Original trace
1				
2				
3				
4				
5				
6				

7				
8				
9				
10				
11				
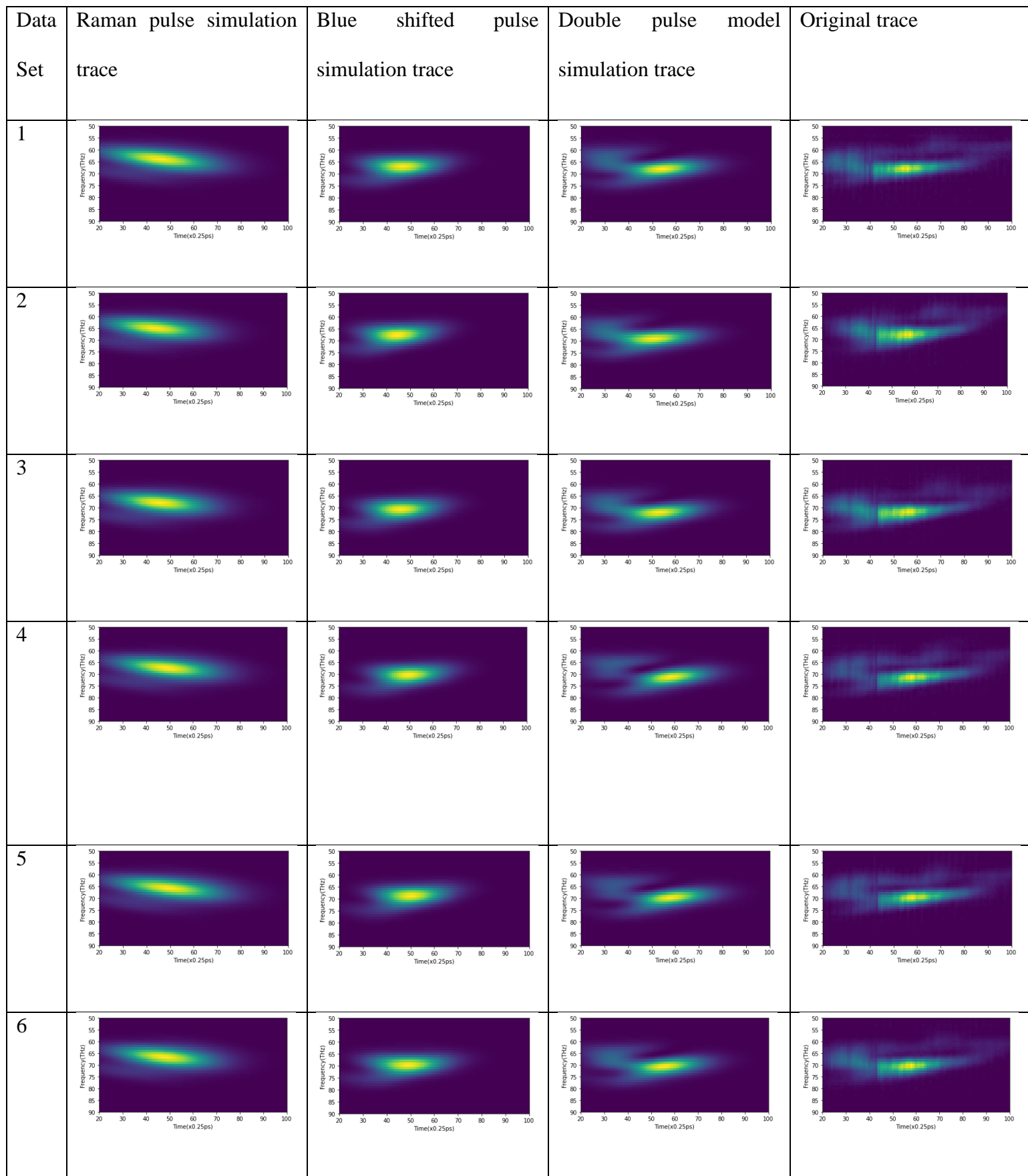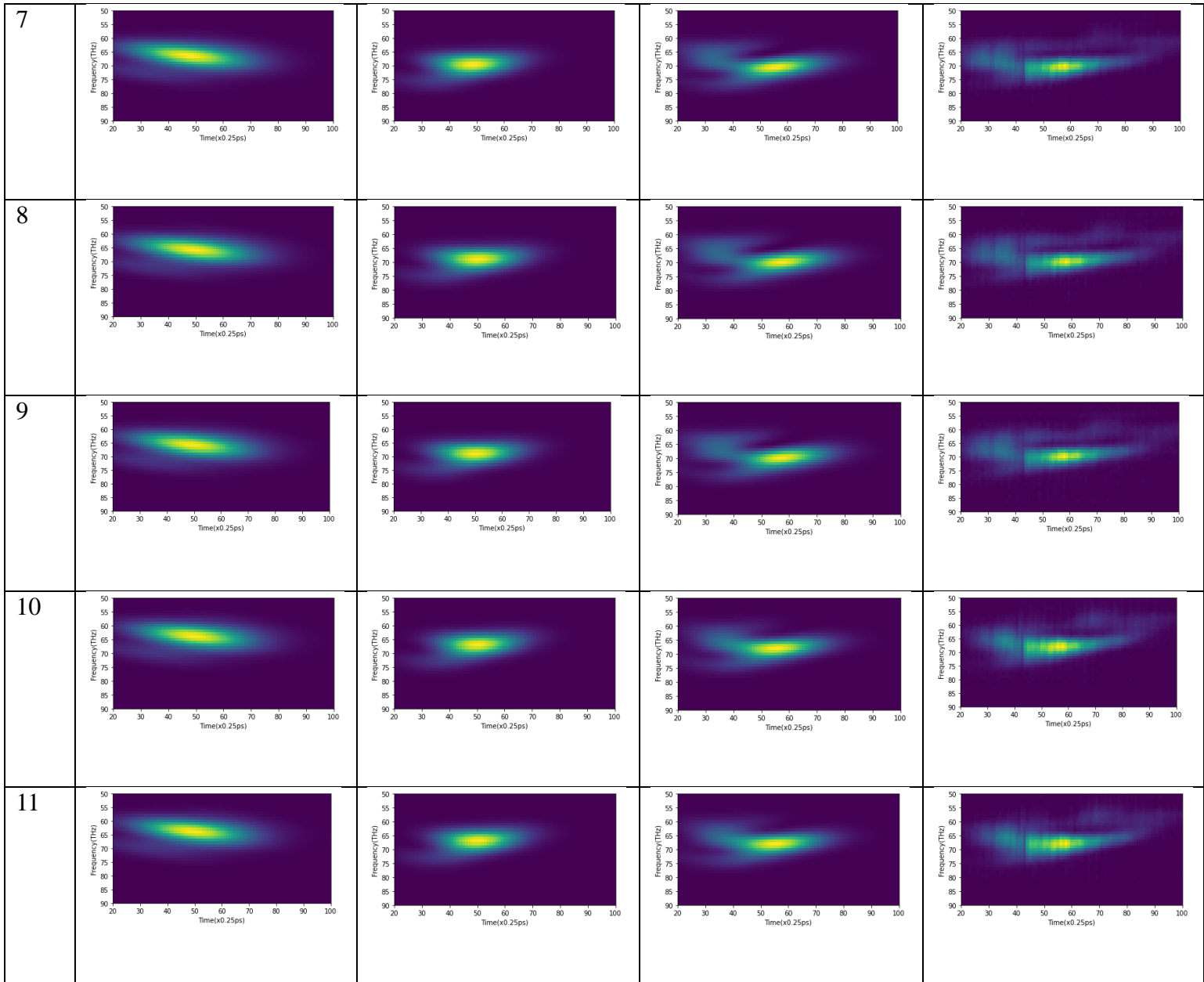
Table 3.2. Simulated and original trace for 11 data set of case B. Unit for x-axis: 46.77109 fs/pixel. Unit for y-axis: 0.1670369 THz/pixel.

Data Set	Raman pulse simulation trace	Red shifted pulse simulation trace	Double pulse model simulation trace	Original trace
1				
2				
3				
4				
5				
6				

7				
8				
9				
10				
11				
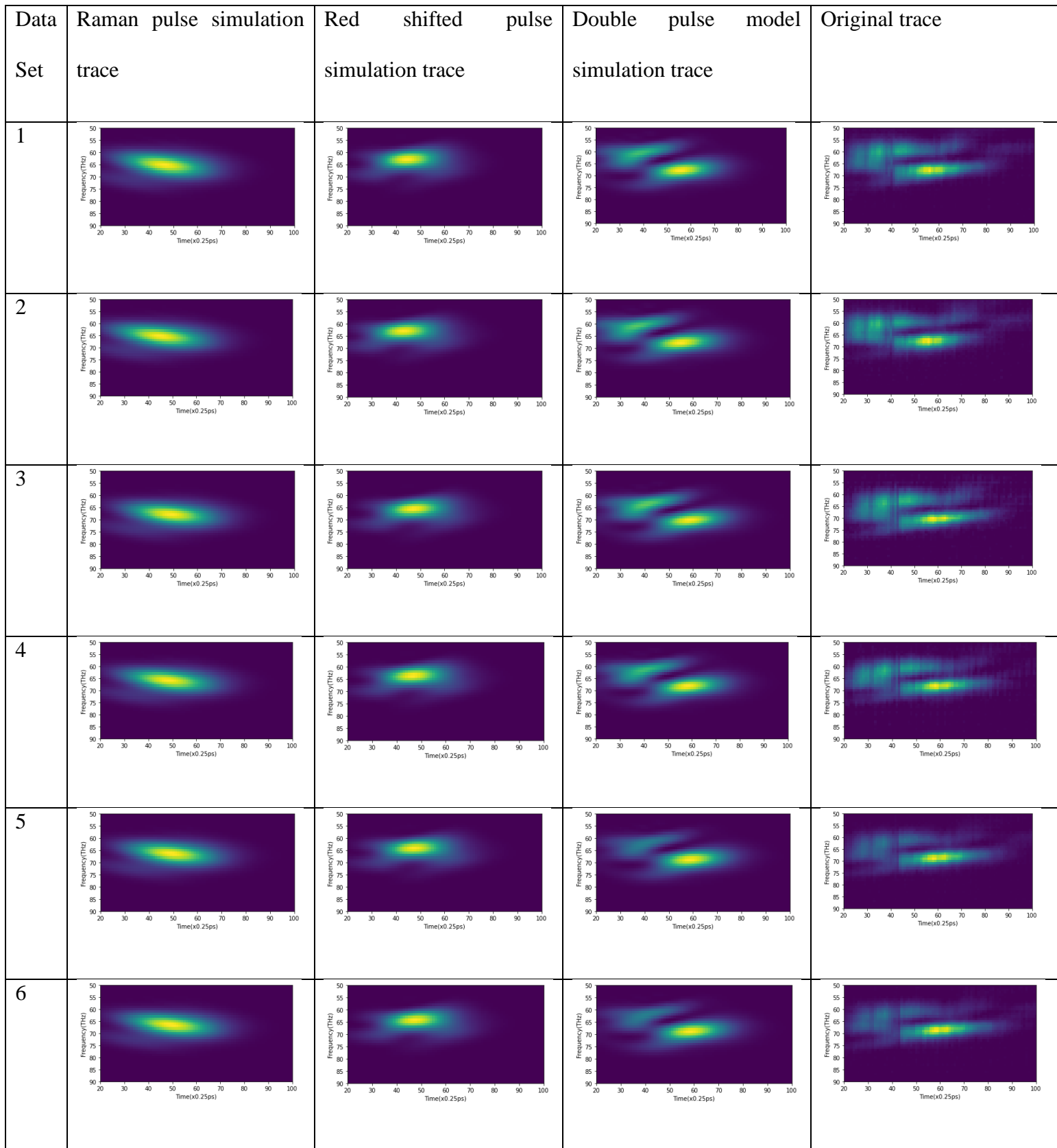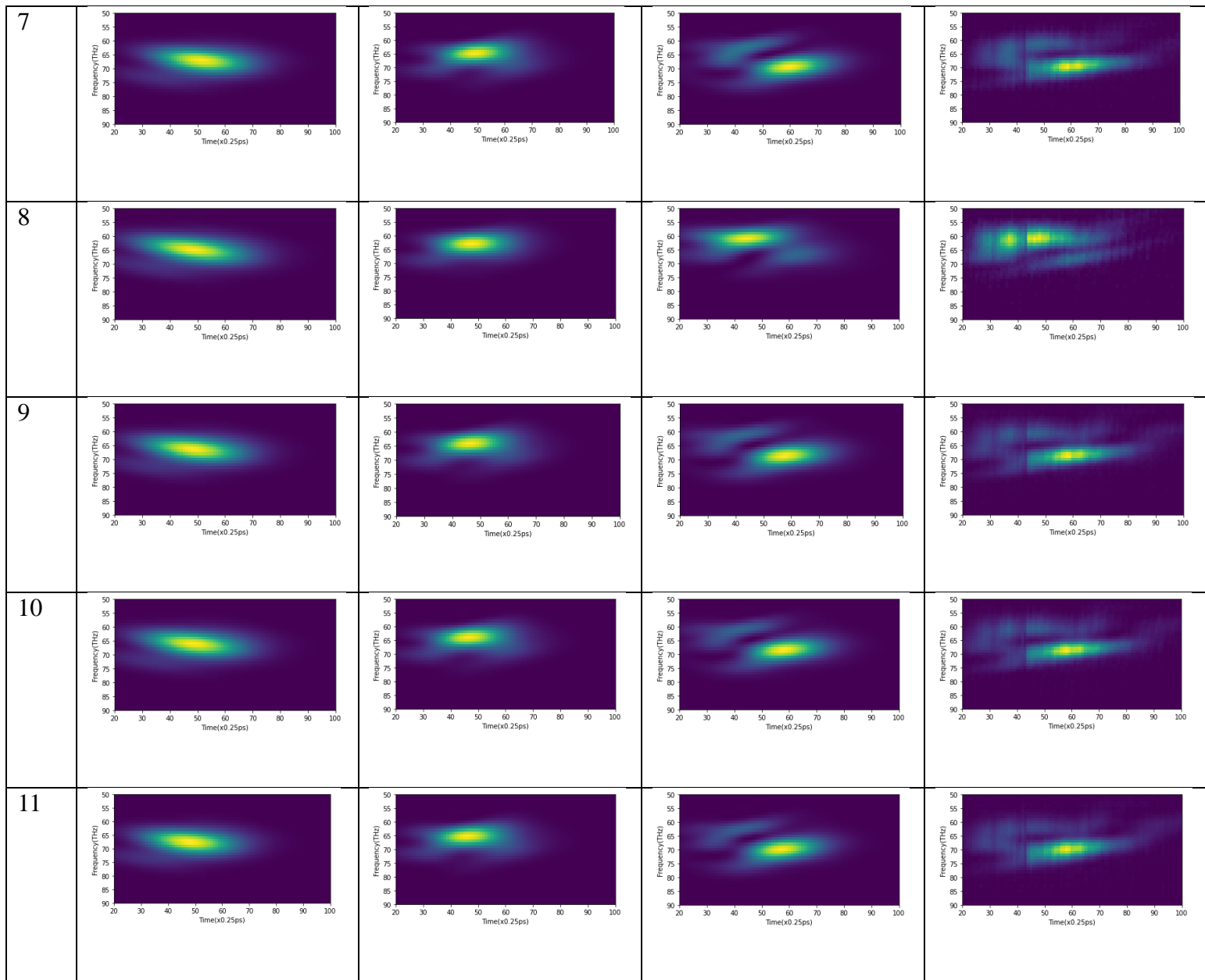
Table 3.3. Simulated and original trace for 11 data set of case C. Unit for x-axis: 46.77109 fs/pixel. Unit for y-axis: 0.1670369 THz/pixel.

Data Set	Raman pulse simulation trace	Red shifted pulse simulation trace	Double pulse model simulation trace	Original trace
1				
2				
3				
4				
5				
6				

7				
8				
9				
10				
11				
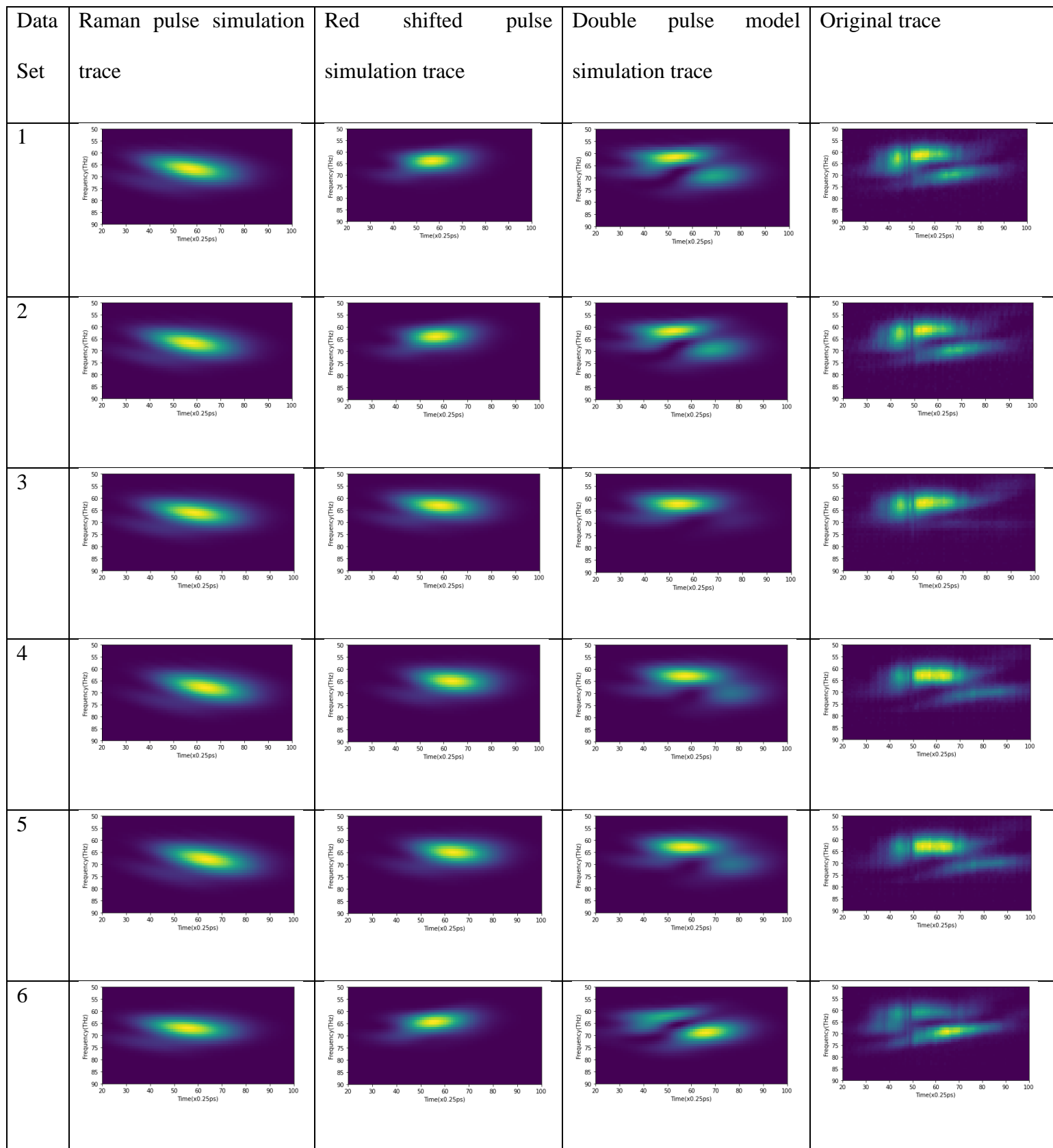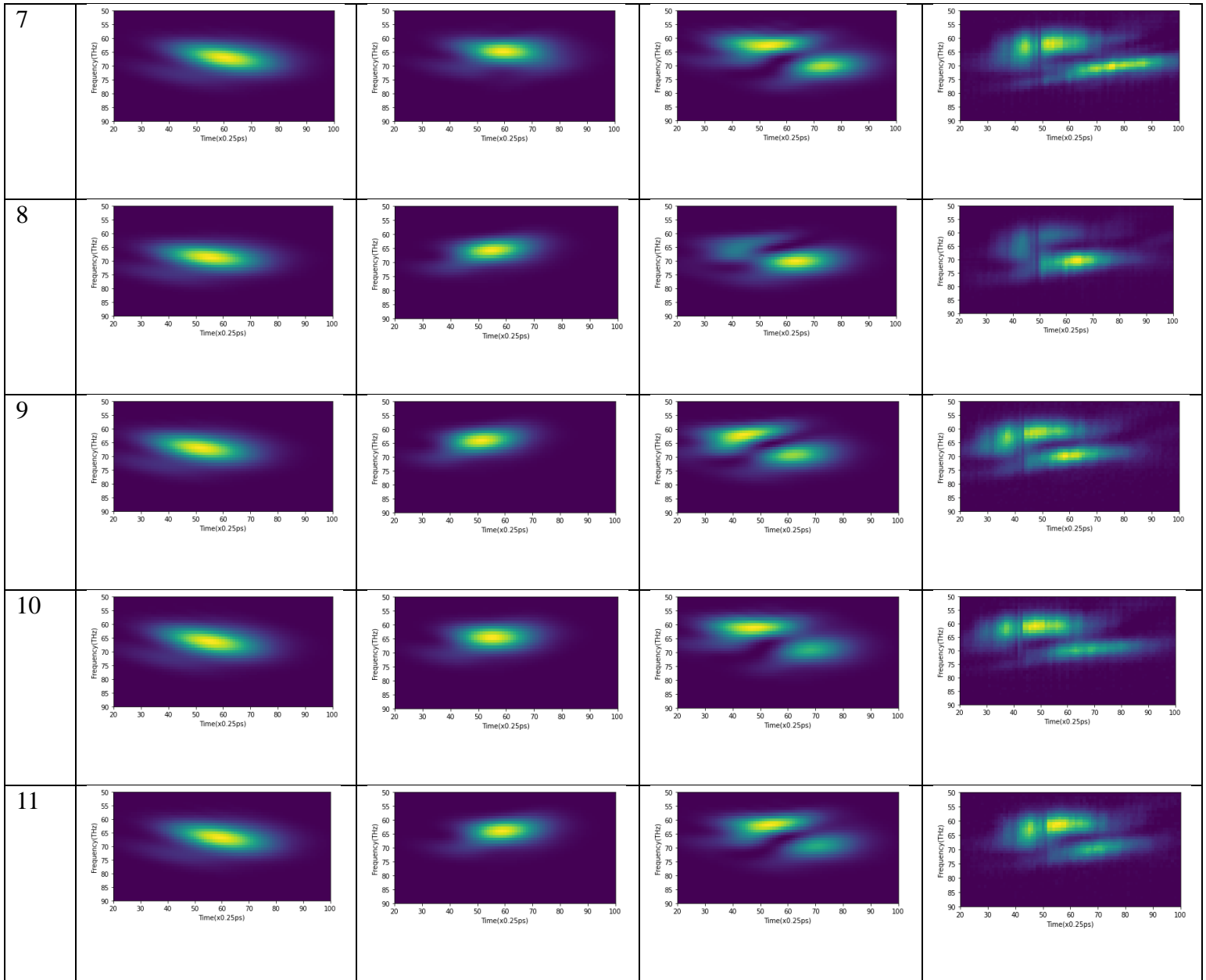
Table 3.4. Simulated and original trace for 11 data set of case D. Unit for x-axis: 46.77109 fs/pixel. Unit for y-axis: 0.1670369 THz/pixel.

Data Set	Raman pulse simulation trace	Red shifted pulse simulation trace	Double pulse model simulation trace	Original trace
1				
2				
3				
4				
5				
6				

7				
8				
9				
10				
11				
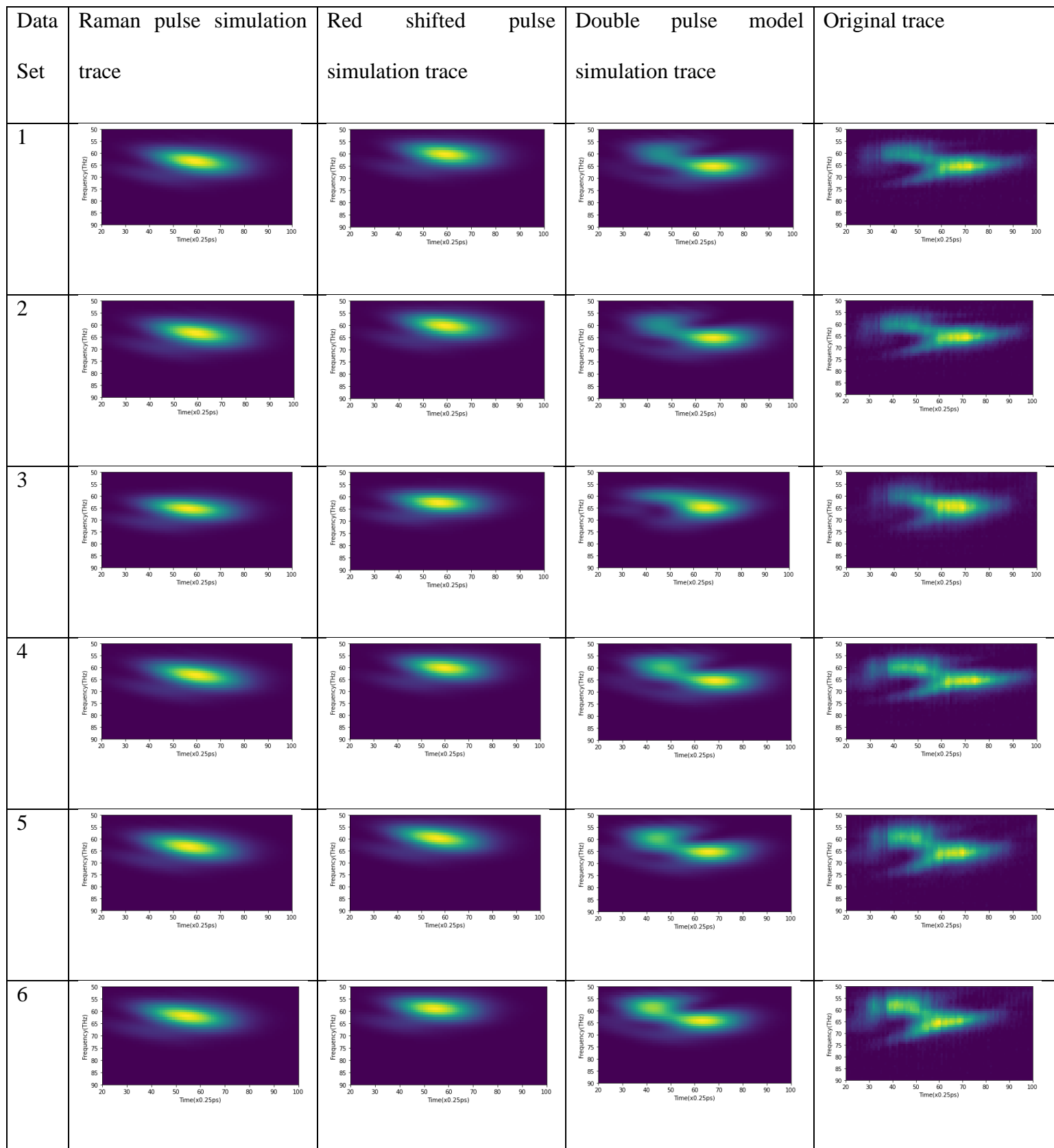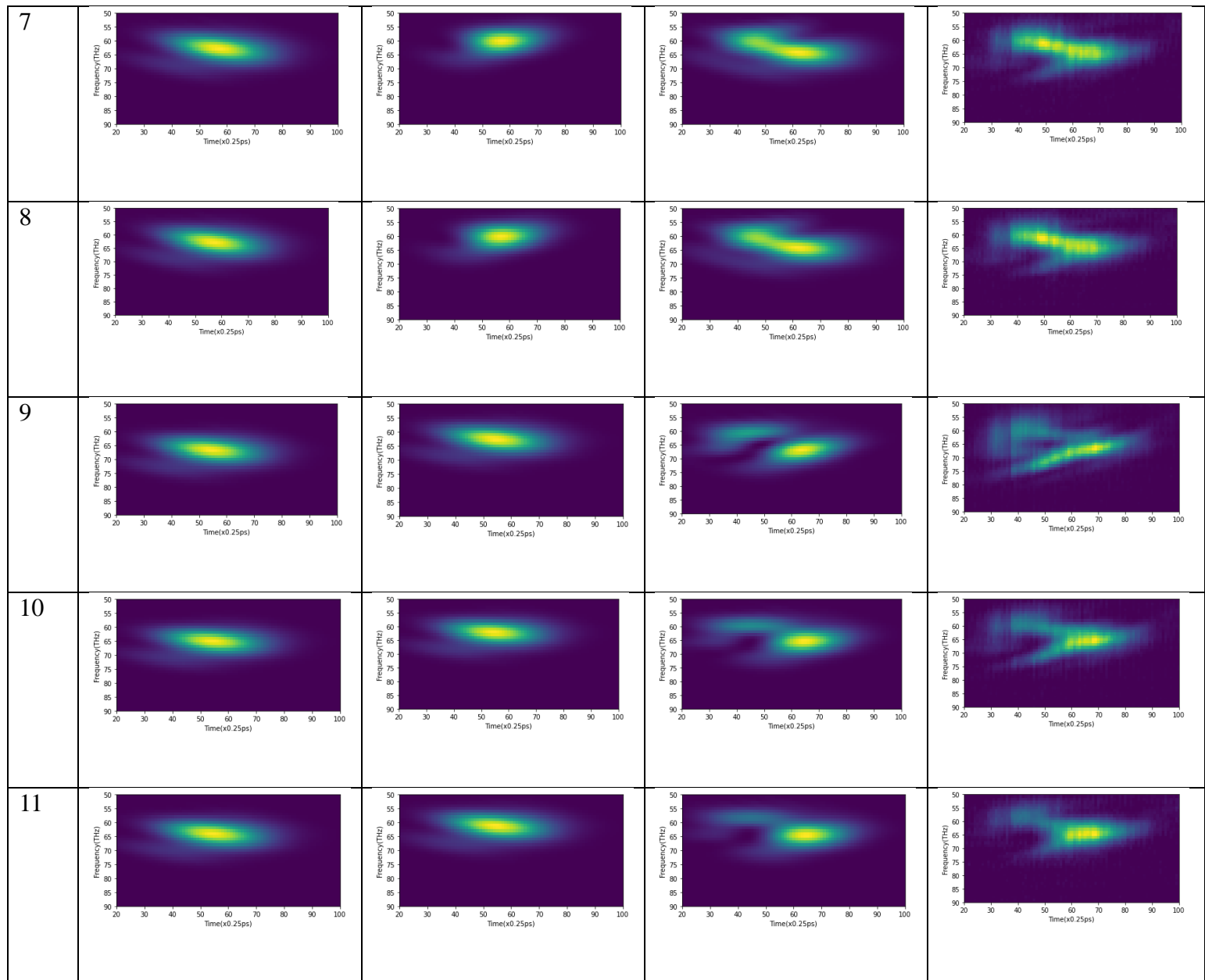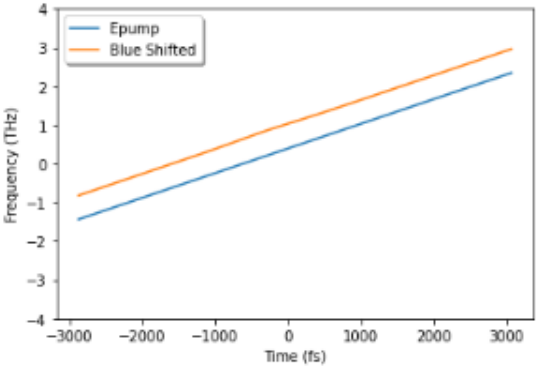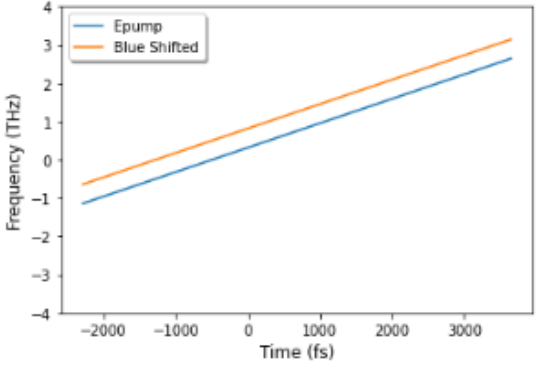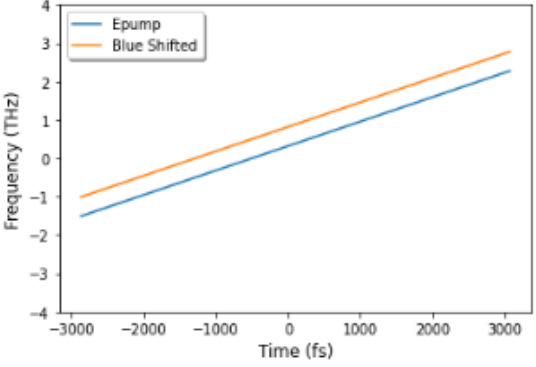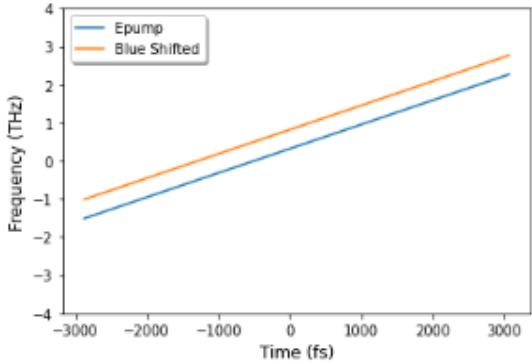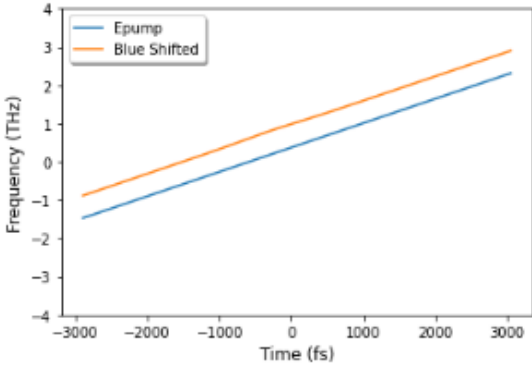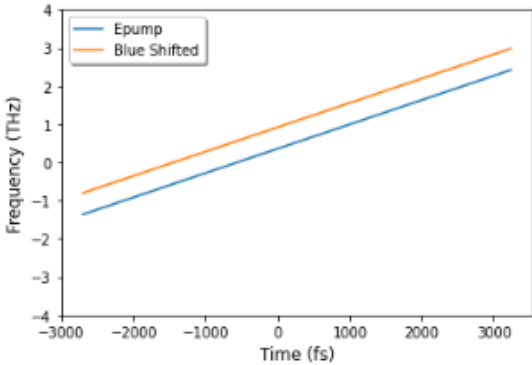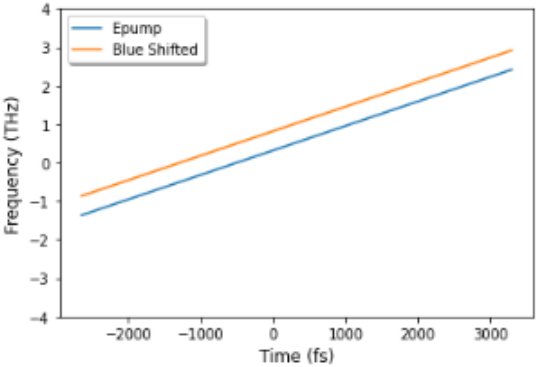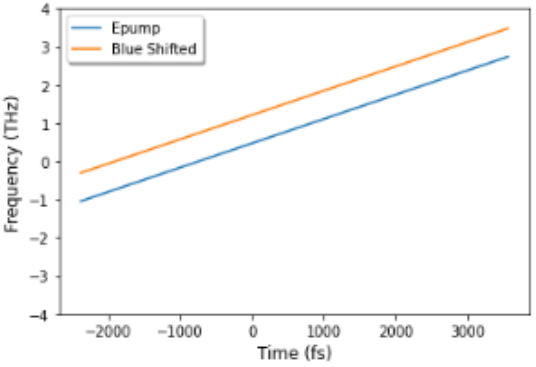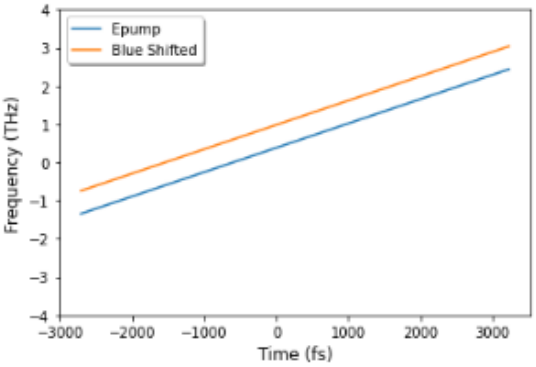
Table 3.5. Simulated and original trace for 11 data set of case E. Unit for x-axis: 46.77109 fs/pixel. Unit for y-axis: 0.1670369 THz/pixel.

In the tables above, the second row shows the simulated trace of the Raman pulse. The third row shows the simulated trace of red or blue shifted shoulder pulse. The fourth row shows the simulated total Raman pulse trace. And the fifth row shows the original trace from the experiment.

Data Set	Parameter	Number	Instantaneous frequency (Blue: Raman pulse. Orange: Blue shifted pulse)
1	Error	0.078	
	T1(fs)	650	
	T2(fs)	2000	
	TT0(fs)	1200	
	tpp(fs)*dd	-618	
	A	3.45	
	a2	0.000004	
	f0	0.00086	
	ph0	-2.47	
	ff	0.0001	
	tt(fs)	2872	
Data Set	Parameter	Average number	Instantaneous frequency (Blue: Raman pulse. Orange: Blue shifted pulse)
2	Error	0.12	
	T1(fs)	1162	
	T2(fs)	2000	
	TT0(fs)	200	
	tpp(fs)*dd	-500	
	A	5.55	
	a2	0.000004	
	f0	0.00021	
	ph0	-3.82	
	ff	0.00001	
	tt(fs)	2291	
Data Set	Parameter	Average number	Instantaneous frequency (Blue: Raman pulse. Orange: Blue shifted pulse)
3	Error	0.057	
	T1(fs)	742	
	T2(fs)	1411	
	TT0(fs)	200	
	tpp(fs)*dd	-500	
	A	2.95	
	a2	0.000004	
	f0	0.00099	
	ph0	-2.21	
	ff	0.0001	
	tt(fs)	2869	

Data Set	Parameter	Average number	Instantaneous frequency (Blue: Raman pulse. Orange: Blue shifted pulse)
4	Error	0.055	
	T1(fs)	773	
	T2(fs)	1370	
	TT0(fs)	200	
	tpp(fs)*dd	-500	
	A	2.85	
	a2	0.000004	
	f0	0.00098	
	ph0	-2.14	
	ff	0.0001	
	tt(fs)	2873	
Data Set	Parameter	Average number	Instantaneous frequency (Blue: Raman pulse. Orange: Blue shifted pulse)
5	Error	0.12	
	T1(fs)	600	
	T2(fs)	2000	
	TT0(fs)	1200	
	tpp(fs)*dd	-586	
	A	2.75	
	a2	0.000004	
	f0	0.00089	
	ph0	-2.55	
	ff	0.0001	
	tt(fs)	2893	
Data Set	Parameter	Average number	Instantaneous frequency (Blue: Raman pulse. Orange: Blue shifted pulse)
6	Error	0.043	
	T1(fs)	789	
	T2(fs)	2000	
	TT0(fs)	200	
	tpp(fs)*dd	-562	
	A	3.55	
	a2	0.000004	
	f0	0.0007	
	ph0	-2.64	
	ff	0.0001	
	tt(fs)	2704	

Data Set	Parameter	Average number	Instantaneous frequency (Blue: Raman pulse. Orange: Blue shifted pulse)
7	Error	0.088	
	T1(fs)	821	
	T2(fs)	2000	
	TT0(fs)	200	
	tpp(fs)*dd	-500	
	A	2.65	
	a2	0.000004	
	f0	0.0008	
	ph0	-2.9	
	ff	0.0001	
	tt(fs)	2646	

Data Set	Parameter	Average number	Instantaneous frequency (Blue: Raman pulse. Orange: Blue shifted pulse)
8	Error	0.069	
	T1(fs)	907	
	T2(fs)	2000	
	TT0(fs)	200	
	tpp(fs)*dd	-740	
	A	2.55	
	a2	0.000004	
	f0	0.0008	
	ph0	-2.71	
	ff	0.0001	
	tt(fs)	2378	

Data Set	Parameter	Average number	Instantaneous frequency (Blue: Raman pulse. Orange: Blue shifted pulse)
9	Error	0.067	
	T1(fs)	657	
	T2(fs)	2000	
	TT0(fs)	200	
	tpp(fs)*dd	-600	
	A	3.15	
	a2	0.000004	
	f0	0.00073	
	ph0	-3.03	
	ff	0.0001	
	tt(fs)	2713	
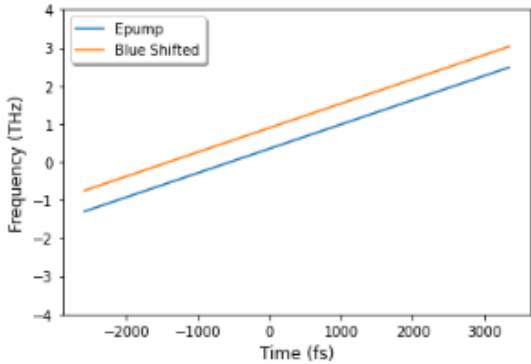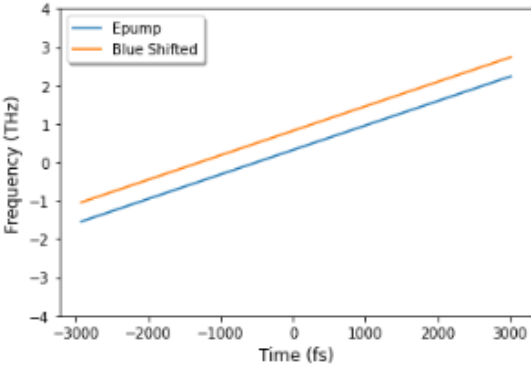
Data Set	Parameter	Average number	Instantaneous frequency (Blue: Raman pulse. Orange: Blue shifted pulse)
10	Error	0.049	
	T1(fs)	837	
	T2(fs)	2000	
	TT0(fs)	200	
	tpp(fs)*dd	-546	
	A	2.65	
	a2	0.000004	
	f0	0.00085	
	ph0	-2.59	
	ff	0.0001	
	tt(fs)	2590	
Data Set	Parameter	Average number	Instantaneous frequency (Blue: Raman pulse. Orange: Blue shifted pulse)
11	Error	0.12	
	T1(fs)	600	
	T2(fs)	2000	
	TT0(fs)	200	
	tpp(fs)*dd	-500	
	A	2.45	
	a2	0.000004	
	f0	-0.00095	
	ph0	-2.41	
	ff	0.0001	
	tt(fs)	2926	

Table 3.6. The data and instantaneous frequency of case A. Left - Simulation results for 11 data sets of case A (666 fs blue shifted pulses). Right - The instantaneous frequency of the Raman pulse and blue shifted pulse.

Data Set	Parameter	Number	Instantaneous frequency (Blue: Raman pulse. Orange: Blue shifted pulse)
1	Error	0.1	
	T1(fs)	1543	
	T2(fs)	836	
	TT0(fs)	1000	
	tpp(fs)*dd	-337	
	A	0.5	
	a2	0.000004	
	f0	0.00008	
	ph0	0.72	
	ff	0.00018	
	tt(fs)	2097	
Data Set	Parameter	Average number	Instantaneous frequency (Blue: Raman pulse. Orange: Blue shifted pulse)
2	Error	0.064	
	T1(fs)	1365	
	T2(fs)	743	
	TT0(fs)	652	
	tpp(fs)*dd	-303	
	A	0.5	
	a2	0.000004	
	f0	0.00026	
	ph0	1.01	
	ff	0.00015	
	tt(fs)	2011	
Data Set	Parameter	Average number	Instantaneous frequency (Blue: Raman pulse. Orange: Blue shifted pulse)
3	Error	0.062	
	T1(fs)	1338	
	T2(fs)	770	
	TT0(fs)	1000	
	tpp(fs)*dd	-370	
	A	0.5	
	a2	0.000004	
	f0	0.00075	
	ph0	0.78	
	ff	0.00013	
	tt(fs)	2085	

Data Set	Parameter	Average number	Instantaneous frequency (Blue: Raman pulse. Orange: Blue shifted pulse)
4	Error	0.089	
	T1(fs)	1382	
	T2(fs)	745	
	TT0(fs)	623	
	tpp(fs)*dd	-351	
	A	0.7	
	a2	0.000004	
	f0	0.00066	
	ph0	1.05	
	ff	0.0002	
	tt(fs)	2244	
Data Set	Parameter	Average number	Instantaneous frequency (Blue: Raman pulse. Orange: Blue shifted pulse)
5	Error	0.085	
	T1(fs)	1507	
	T2(fs)	771	
	TT0(fs)	805	
	tpp(fs)*dd	-347	
	A	0.6	
	a2	0.000004	
	f0	0.00038	
	ph0	1	
	ff	0.0002	
	tt(fs)	2261	
Data Set	Parameter	Average number	Instantaneous frequency (Blue: Raman pulse. Orange: Blue shifted pulse)
6	Error	0.062	
	T1(fs)	1358	
	T2(fs)	863	
	TT0(fs)	924	
	tpp(fs)*dd	-315	
	A	0.5	
	a2	0.000004	
	f0	0.00053	
	ph0	0.98	
	ff	0.0002	
	tt(fs)	2188	

Data Set	Parameter	Average number	Instantaneous frequency (Blue: Raman pulse. Orange: Blue shifted pulse)
7	Error	0.066	
	T1(fs)	1422	
	T2(fs)	804	
	TT0(fs)	1000	
	tpp(fs)*dd	-370	
	A	0.5	
	a2	0.000004	
	f0	0.0005	
	ph0	0.8	
	ff	0.00018	
	tt(fs)	2188	

Data Set	Parameter	Average number	Instantaneous frequency (Blue: Raman pulse. Orange: Blue shifted pulse)
8	Error	0.082	
	T1(fs)	1418	
	T2(fs)	849	
	TT0(fs)	923	
	tpp(fs)*dd	-370	
	A	0.5	
	a2	0.000004	
	f0	0.00039	
	ph0	1.02	
	ff	0.0002	
	tt(fs)	2257	

Data Set	Parameter	Average number	Instantaneous frequency (Blue: Raman pulse. Orange: Blue shifted pulse)
9	Error	0.079	
	T1(fs)	1407	
	T2(fs)	848	
	TT0(fs)	868	
	tpp(fs)*dd	-370	
	A	0.5	
	a2	0.000004	
	f0	0.0006	
	ph0	0.99	
	ff	0.0002	
	tt(fs)	2261	

Data Set	Parameter	Average number	Instantaneous frequency (Blue: Raman pulse. Orange: Blue shifted pulse)
10	Error	0.054	
	T1(fs)	1353	
	T2(fs)	758	
	TT0(fs)	1000	
	tpp(fs)*dd	-370	
	A	0.4	
	a2	0.000004	
	f0	0.00006	
	ph0	1.13	
	ff	0.00012	
	tt(fs)	2272	
Data Set	Parameter	Average number	Instantaneous frequency (Blue: Raman pulse. Orange: Blue shifted pulse)
11	Error	0.055	
	T1(fs)	1347	
	T2(fs)	759	
	TT0(fs)	1000	
	tpp(fs)*dd	-370	
	A	0.4	
	a2	0.000004	
	f0	0.00006	
	ph0	1.12	
	ff	0.00012	
	tt(fs)	2271	

Table 3.7. The data and instantaneous frequency of case B. Left - Simulation results for 11 data sets of case B (333 fs blue shifted pulses). Right - The instantaneous frequency of the Raman pulse and blue shifted pulse.
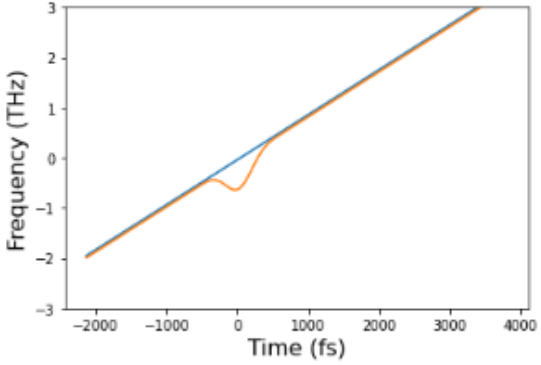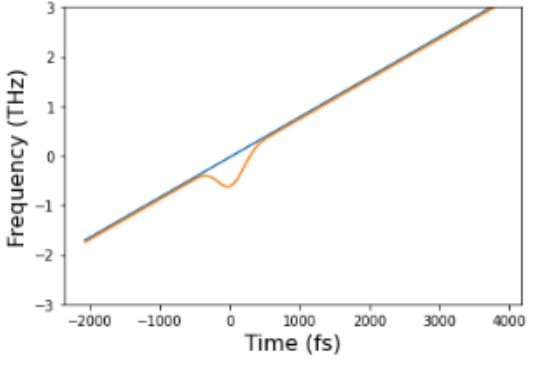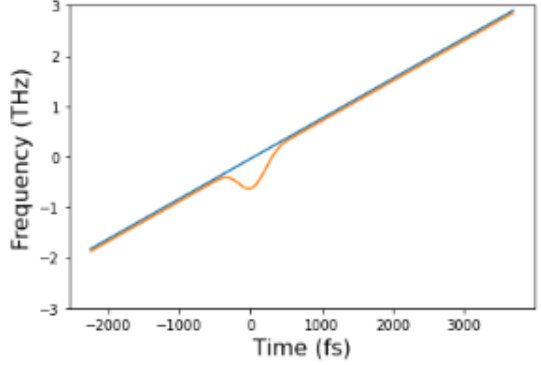
Data Set	Parameter	Number	Instantaneous frequency (Blue: Raman pulse. Orange: Red shifted pulse)
1	Error	0.11	
	T1(fs)	1134	
	T2(fs)	850	
	TT0(fs)	437	
	tpp(fs)*dd	42	
	A	1.11	
	a2	0.00000564	
	f0	0.00029	
	ph0	-2.06	
	ff	0.000266	
	tt(fs)	2133	
Data Set	Parameter	Average number	Instantaneous frequency (Blue: Raman pulse. Orange: Red shifted pulse)
2	Error	0.11	
	T1(fs)	1205	
	T2(fs)	900	
	TT0(fs)	441	
	tpp(fs)*dd	41	
	A	1.11	
	a2	0.00000509	
	f0	0.0003	
	ph0	-2.07	
	ff	0.000266	
	tt(fs)	2068	
Data Set	Parameter	Average number	Instantaneous frequency (Blue: Raman pulse. Orange: Red shifted pulse)
3	Error	0.12	
	T1(fs)	1139	
	T2(fs)	879	
	TT0(fs)	444	
	tpp(fs)*dd	50	
	A	1.11	
	a2	0.000005	
	f0	0.00073	
	ph0	-2.06	
	ff	0.000266	
	tt(fs)	2248	

Data Set	Parameter	Average number	Instantaneous frequency (Blue: Raman pulse. Orange: Red shifted pulse)
4	Error	0.11	
	T1(fs)	1164	
	T2(fs)	893	
	TT0(fs)	444	
	tpp(fs)*dd	47	
	A	1.11	
	a2	0.000005	
	f0	0.0004	
	ph0	-2.06	
	ff	0.000266	
	tt(fs)	2220	
Data Set	Parameter	Average number	Instantaneous frequency (Blue: Raman pulse. Orange: Red shifted pulse)
5	Error	0.11	
	T1(fs)	1139	
	T2(fs)	941	
	TT0(fs)	436	
	tpp(fs)*dd	65	
	A	1.21	
	a2	0.000005	
	f0	0.00049	
	ph0	-1.95	
	ff	0.000266	
	tt(fs)	2265	
Data Set	Parameter	Average number	Instantaneous frequency (Blue: Raman pulse. Orange: Red shifted pulse)
6	Error	0.11	
	T1(fs)	1155	
	T2(fs)	907	
	TT0(fs)	459	
	tpp(fs)*dd	28	
	A	1.21	
	a2	0.000005	
	f0	0.00051	
	ph0	-2	
	ff	0.00026	
	tt(fs)	2268	
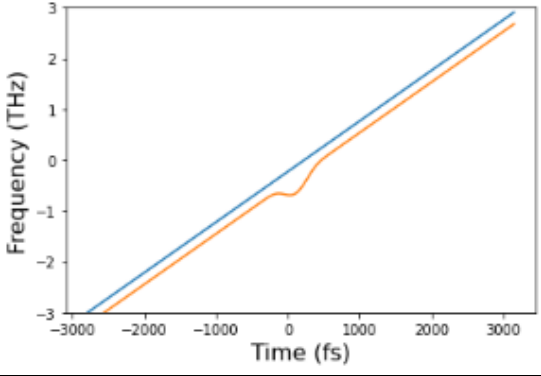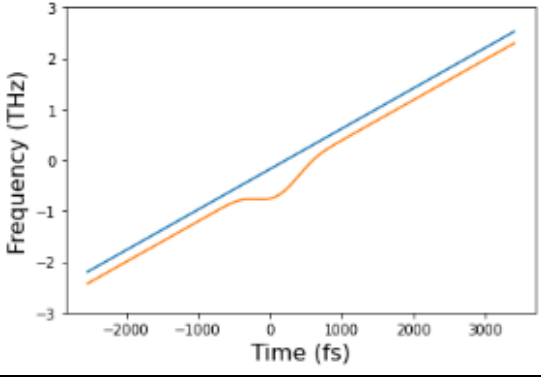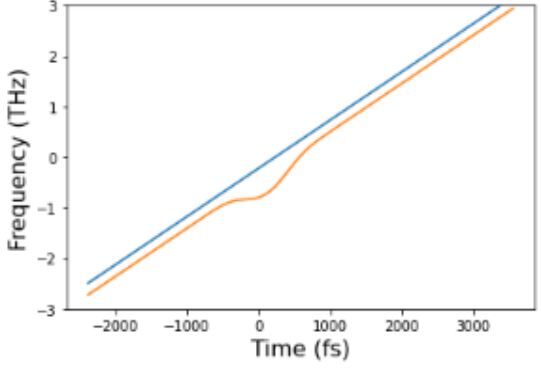
Data Set	Parameter	Average number	Instantaneous frequency (Blue: Raman pulse. Orange: Red shifted pulse)
7	Error	0.083	
	T1(fs)	1073	
	T2(fs)	917	
	TT0(fs)	461	
	tpp(fs)*dd	2	
	A	1.21	
	a2	0.000005	
	f0	0.00061	
	ph0	-2	
	ff	0.000266	
	tt(fs)	2357	

Data Set	Parameter	Average number	Instantaneous frequency (Blue: Raman pulse. Orange: Red shifted pulse)
8	Error	0.086	
	T1(fs)	1246	
	T2(fs)	815	
	TT0(fs)	676	
	tpp(fs)*dd	100	
	A	0.61	
	a2	0.000005	
	f0	0.00024	
	ph0	-2.1	
	ff	0.00017	
	tt(fs)	2226	

Data Set	Parameter	Average number	Instantaneous frequency (Blue: Raman pulse. Orange: Red shifted pulse)
9	Error	0.1	
	T1(fs)	1139	
	T2(fs)	907	
	TT0(fs)	453	
	tpp(fs)*dd	24	
	A	1.11	
	a2	0.000005	
	f0	0.00049	
	ph0	-1.91	
	ff	0.000265	
	tt(fs)	2220	

Data Set	Parameter	Average number	Instantaneous frequency (Blue: Raman pulse. Orange: Red shifted pulse)
10	Error	0.1	
	T1(fs)	1136	
	T2(fs)	916	
	TT0(fs)	450	
	tpp(fs)*dd	26	
	A	1.11	
	a2	0.000005	
	f0	0.00045	
	ph0	-1.94	
	ff	0.00026	
	tt(fs)	2232	
Data Set	Parameter	Average number	Instantaneous frequency (Blue: Raman pulse. Orange: Red shifted pulse)
11	Error	0.077	
	T1(fs)	1040	
	T2(fs)	944	
	TT0(fs)	435	
	tpp(fs)*dd	59	
	A	1.11	
	a2	0.000005	
	f0	0.00067	
	ph0	-1.85	
	ff	0.000265	
	tt(fs)	2199	

Table 3.8. The data and instantaneous frequency of case C. Left - Simulation results for 11 data sets of case C (timed together pulses). Right - The instantaneous frequency of the Raman pulse and red shifted pulse.
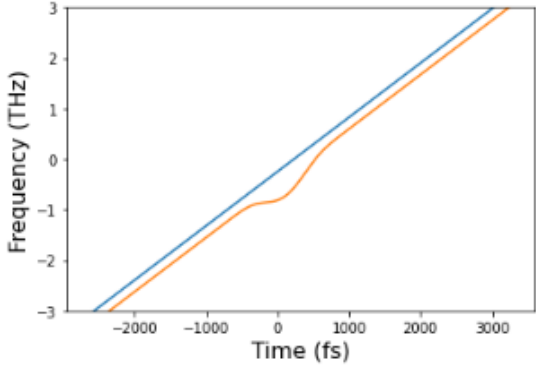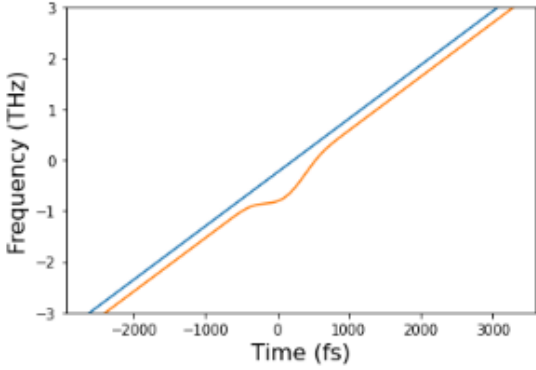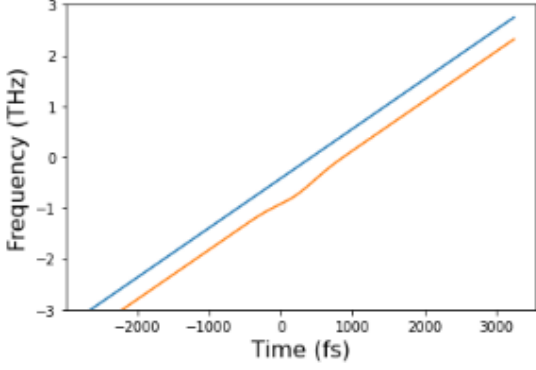
Data Set	Parameter	Number	Instantaneous frequency (Blue: Raman pulse. Orange: Red shifted pulse)
1	Error	0.089	
	T1(fs)	1100	
	T2(fs)	701	
	TT0(fs)	729	
	tpp(fs)*dd	230	
	A	0.7	
	a2	0.00000675	
	f0	0.00056	
	ph0	4.03	
	ff	0.000266	
	tt(fs)	2647	
Data Set	Parameter	Average number	Instantaneous frequency (Blue: Raman pulse. Orange: Red shifted pulse)
2	Error	0.087	
	T1(fs)	1100	
	T2(fs)	700	
	TT0(fs)	746	
	tpp(fs)*dd	230	
	A	0.7	
	a2	0.00000664	
	f0	0.00057	
	ph0	4.05	
	ff	0.000266	
	tt(fs)	2644	
Data Set	Parameter	Average number	Instantaneous frequency (Blue: Raman pulse. Orange: Red shifted pulse)
3	Error	0.072	
	T1(fs)	1100	
	T2(fs)	996	
	TT0(fs)	800	
	tpp(fs)*dd	430	
	A	0.4	
	a2	0.00000613	
	f0	0.00045	
	ph0	2.89	
	ff	0.00018	
	tt(fs)	2694	
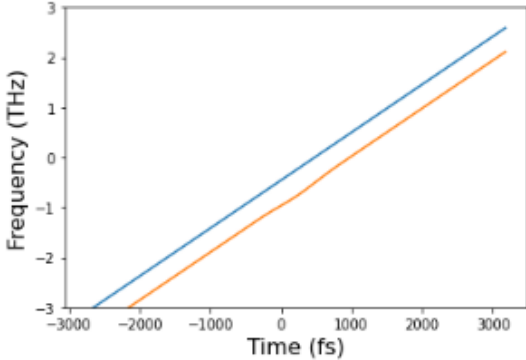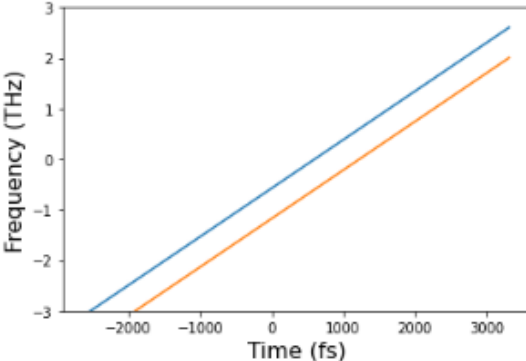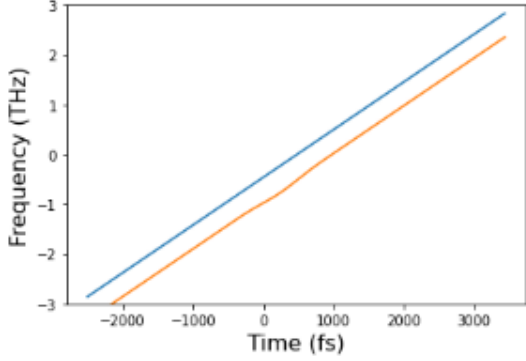
Data Set	Parameter	Average number	Instantaneous frequency (Blue: Raman pulse. Orange: Red shifted pulse)
4	Error	0.054	
	T1(fs)	1100	
	T2(fs)	872	
	TT0(fs)	850	
	tpp(fs)*dd	430	
	A	0.5	
	a2	0.00000708	
	f0	0.00074	
	ph0	2.9	
	ff	0.00016	
	tt(fs)	2936	

Data Set	Parameter	Average number	Instantaneous frequency (Blue: Raman pulse. Orange: Red shifted pulse)
5	Error	0.054	
	T1(fs)	1100	
	T2(fs)	880	
	TT0(fs)	850	
	tpp(fs)*dd	430	
	A	0.5	
	a2	0.00000708	
	f0	0.00074	
	ph0	2.89	
	ff	0.000166	
	tt(fs)	2937	

Data Set	Parameter	Average number	Instantaneous frequency (Blue: Raman pulse. Orange: Red shifted pulse)
6	Error	0.14	
	T1(fs)	1100	
	T2(fs)	746	
	TT0(fs)	655	
	tpp(fs)*dd	230	
	A	1	
	a2	0.00000479	
	f0	0.0006	
	ph0	4.43	
	ff	0.000266	
	tt(fs)	2569	
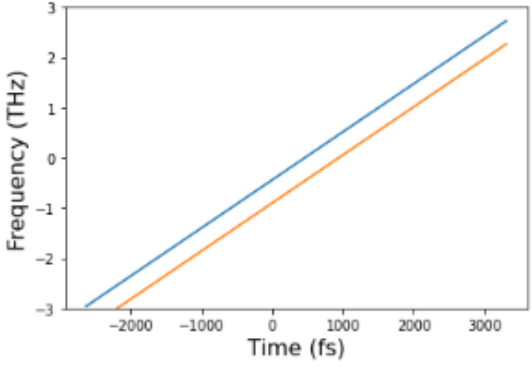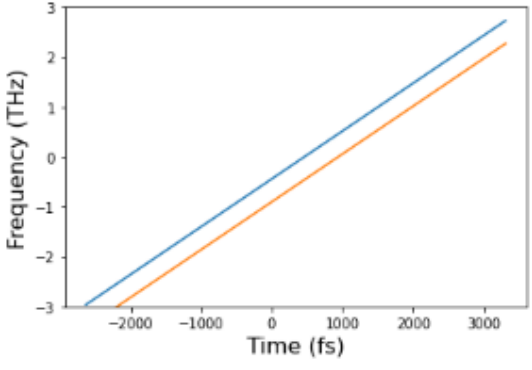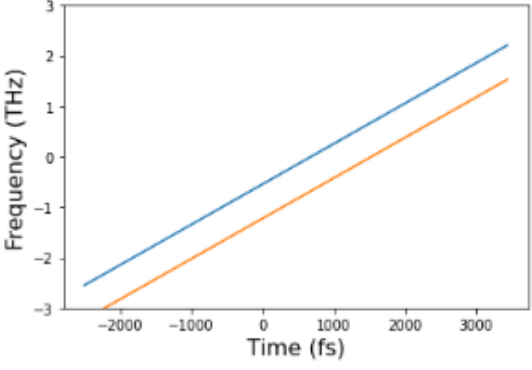
Data Set	Parameter	Average number	Instantaneous frequency (Blue: Raman pulse. Orange: Red shifted pulse)
7	Error	0.13	
	T1(fs)	1100	
	T2(fs)	1000	
	TT0(fs)	432	
	tpp(fs)*dd	230	
	A	0.8	
	a2	0.00000625	
	f0	0.00061	
	ph0	3.42	
	ff	0.000266	
	tt(fs)	2790	

Data Set	Parameter	Average number	Instantaneous frequency (Blue: Raman pulse. Orange: Red shifted pulse)
8	Error	0.1	
	T1(fs)	1100	
	T2(fs)	711	
	TT0(fs)	800	
	tpp(fs)*dd	230	
	A	1.5	
	a2	0.000005	
	f0	0.00087	
	ph0	4.73	
	ff	0.000266	
	tt(fs)	2537	

Data Set	Parameter	Average number	Instantaneous frequency (Blue: Raman pulse. Orange: Red shifted pulse)
9	Error	0.11	
	T1(fs)	1100	
	T2(fs)	659	
	TT0(fs)	800	
	tpp(fs)*dd	230	
	A	1	
	a2	0.00000599	
	f0	0.0006	
	ph0	4.78	
	ff	0.000266	
	tt(fs)	2385	

Data Set	Parameter	Average number	Instantaneous frequency (Blue: Raman pulse. Orange: Red shifted pulse)
10	Error	0.092	
	T1(fs)	1100	
	T2(fs)	734	
	TT0(fs)	443	
	tpp(fs)*dd	230	
	A	0.8	
	a2	0.00000655	
	f0	0.00048	
	ph0	3.88	
	ff	0.00017	
	tt(fs)	2546	
Data Set	Parameter	Average number	Instantaneous frequency (Blue: Raman pulse. Orange: Red shifted pulse)
11	Error	0.089	
	T1(fs)	1100	
	T2(fs)	694	
	TT0(fs)	690	
	tpp(fs)*dd	230	
	A	0.8	
	a2	0.00000638	
	f0	0.00056	
	ph0	3.63	
	ff	0.000266	
	tt(fs)	2738	

Table 3.9. The data and instantaneous frequency of case D. Left - Simulation results for 11 data sets of case D (333 fs red shifted pulses). Right - The instantaneous frequency of the Raman pulse and red shifted pulse.

Data Set	Parameter	Number	Instantaneous frequency (Blue: Raman pulse. Orange: Red shifted pulse)
1	Error	0.045	
	T1(fs)	1104	
	T2(fs)	1000	
	TT0(fs)	800	
	tpp(fs)*dd	514	
	A	2.4	
	a2	0.00000601	
	f0	0.00047	
	ph0	5.39	
	ff	0.000003	
	tt(fs)	2646	
Data Set	Parameter	Average number	Instantaneous frequency (Blue: Raman pulse. Orange: Red shifted pulse)
2	Error	0.045	
	T1(fs)	1108	
	T2(fs)	1000	
	TT0(fs)	800	
	tpp(fs)*dd	530	
	A	2.4	
	a2	0.00000602	
	f0	0.00046	
	ph0	4.07	
	ff	0.000003	
	tt(fs)	2737	
Data Set	Parameter	Average number	Instantaneous frequency (Blue: Raman pulse. Orange: Red shifted pulse)
3	Error	0.024	
	T1(fs)	1100	
	T2(fs)	1033	
	TT0(fs)	421	
	tpp(fs)*dd	460	
	A	0.41	
	a2	0.00000466	
	f0	0.00031	
	ph0	5.02	
	ff	0.000133	
	tt(fs)	2601	

Data Set	Parameter	Average number	Instantaneous frequency (Blue: Raman pulse. Orange: Red shifted pulse)
4	Error	0.064	
	T1(fs)	1160	
	T2(fs)	1000	
	TT0(fs)	800	
	tpp(fs)*dd	478	
	A	2.4	
	a2	0.00000602	
	f0	-0.00002	
	ph0	3.68	
	ff	0.000136	
	tt(fs)	2761	
Data Set	Parameter	Average number	Instantaneous frequency (Blue: Raman pulse. Orange: Red shifted pulse)
5	Error	0.059	
	T1(fs)	1134	
	T2(fs)	1100	
	TT0(fs)	800	
	tpp(fs)*dd	600	
	A	2.4	
	a2	0.00000602	
	f0	-0.00002	
	ph0	4.28	
	ff	0.00002	
	tt(fs)	2623	
Data Set	Parameter	Average number	Instantaneous frequency (Blue: Raman pulse. Orange: Red shifted pulse)
6	Error	0.088	
	T1(fs)	1100	
	T2(fs)	950	
	TT0(fs)	800	
	tpp(fs)*dd	478	
	A	2.2	
	a2	0.00000602	
	f0	-0.00024	
	ph0	4.42	
	ff	0.000153	
	tt(fs)	2505	

Data Set	Parameter	Average number	Instantaneous frequency (Blue: Raman pulse. Orange: Red shifted pulse)
7	Error	0.027	
	T1(fs)	1100	
	T2(fs)	600	
	TT0(fs)	800	
	tpp(fs)*dd	460	
	A	2.8	
	a2	0.00000602	
	f0	-0.00011	
	ph0	3.85	
	ff	0.0000133	
	tt(fs)	2630	

Data Set	Parameter	Average number	Instantaneous frequency (Blue: Raman pulse. Orange: Red shifted pulse)
8	Error	0.028	
	T1(fs)	1100	
	T2(fs)	600	
	TT0(fs)	800	
	tpp(fs)*dd	460	
	A	2.8	
	a2	0.00000602	
	f0	-0.00011	
	ph0	3.99	
	ff	0.0000133	
	tt(fs)	2631	

Data Set	Parameter	Average number	Instantaneous frequency (Blue: Raman pulse. Orange: Red shifted pulse)
9	Error	0.15	
	T1(fs)	1100	
	T2(fs)	1100	
	TT0(fs)	610	
	tpp(fs)*dd	680	
	A	0.81	
	a2	0.00000503	
	f0	0.00054	
	ph0	5.65	
	ff	0.000003	
	tt(fs)	2502	
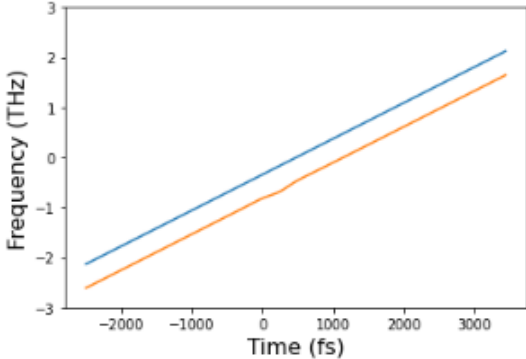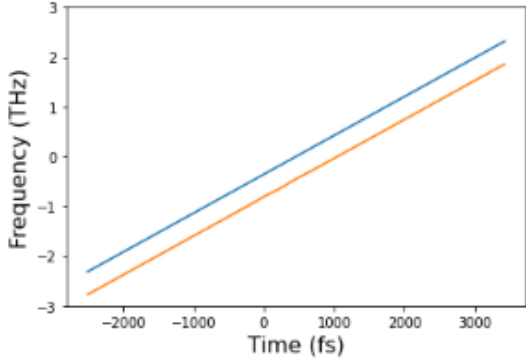
Data Set	Parameter	Average number	Instantaneous frequency (Blue: Raman pulse. Orange: Red shifted pulse)
10	Error	0.051	
	T1(fs)	1100	
	T2(fs)	1072	
	TT0(fs)	601	
	tpp(fs)*dd	538	
	A	0.61	
	a2	0.0000045	
	f0	0.00027	
	ph0	5.15	
	ff	0.000133	
	tt(fs)	2501	
Data Set	Parameter	Average number	Instantaneous frequency (Blue: Raman pulse. Orange: Red shifted pulse)
11	Error	0.031	
	T1(fs)	1100	
	T2(fs)	1100	
	TT0(fs)	266	
	tpp(fs)*dd	460	
	A	0.61	
	a2	0.0000049	
	f0	0.0001	
	ph0	5.16	
	ff	0.000133	
	tt(fs)	2511	

Table 3.10. The data and instantaneous frequency of case E. Left - Simulation results for 11 data sets of case E (666fs red shifted pulses). Right - The instantaneous frequency of the Raman pulse and red shifted pulse.

The instantaneous frequency and data of simulation are shown in Table 3.1 to 3.10 above. T1 is the pulse duration of the Raman pulse. T2 is the pulse duration of the red shifted pulse. TT0 is the pulse duration of the generalized Rabi frequency. The tpp*dd

is the time jitter. A is the amplitude ratio between Raman pulse and red shifted pulse. The a2 is the slope coefficient of the linear chirp in the instantaneous frequency. The f0 is the center frequency. The ph0 is the pi phase shift. The ff is the amplitude coefficient of the generalized Rabi frequency. The tt is the time delay.

From the tables above, the instantaneous frequency of the Raman pulse is linear chirp. The instantaneous frequency of the blue shifted pulse is the linear chirp with a gaussian peak in the middle, while the instantaneous frequency of the red shifted pulse is the linear chirp with a gaussian dip in the middle. The dips or peaks become smaller when the constant detuning becomes bigger. And the case C shows the biggest dip in the middle. From the theory, the constant detuning in the instantaneous frequency should be almost 0 for the case C. The constant detuning for the case B and D should be around 333 fs in time domain. The constant detuning for case A and E should be around 666 fs in time domain.

Case	A	B	C	D	E
Error	0.078	0.072	0.101	0.092	0.055
T1(fs)	776	1403	1142	1100	1109
T2(fs)	1889	795	897	790	959
TT0(fs)	382	890	467	708	681
tpp*dd	-559	-352	44	284	514
A	3.14	0.51	1.09	0.79	1.8
a2	$4.0*10^{-6}$	$4.0*10^{-6}$	$5.07*10^{-6}$	$6.24*10^{-6}$	$5.56*10^{-6}$
f0	$6.24*10^{-4}$	$3.8*10^{-4}$	$4.7*10^{-4}$	$6.16*10^{-4}$	$1.5*10^{-4}$
ph0	-2.68	0.96	-2	3.78	4.6
ff	$0.92*10^{-4}$	$1.7*10^{-4}$	$2.56*10^{-4}$	$2.3*10^{-4}$	$0.67*10^{-4}$
tt(fs)	2705	2194	2221	2674	2604

Table 3.11. The average data of 11 simulated traces from the double pulse model simulation program for five cases.
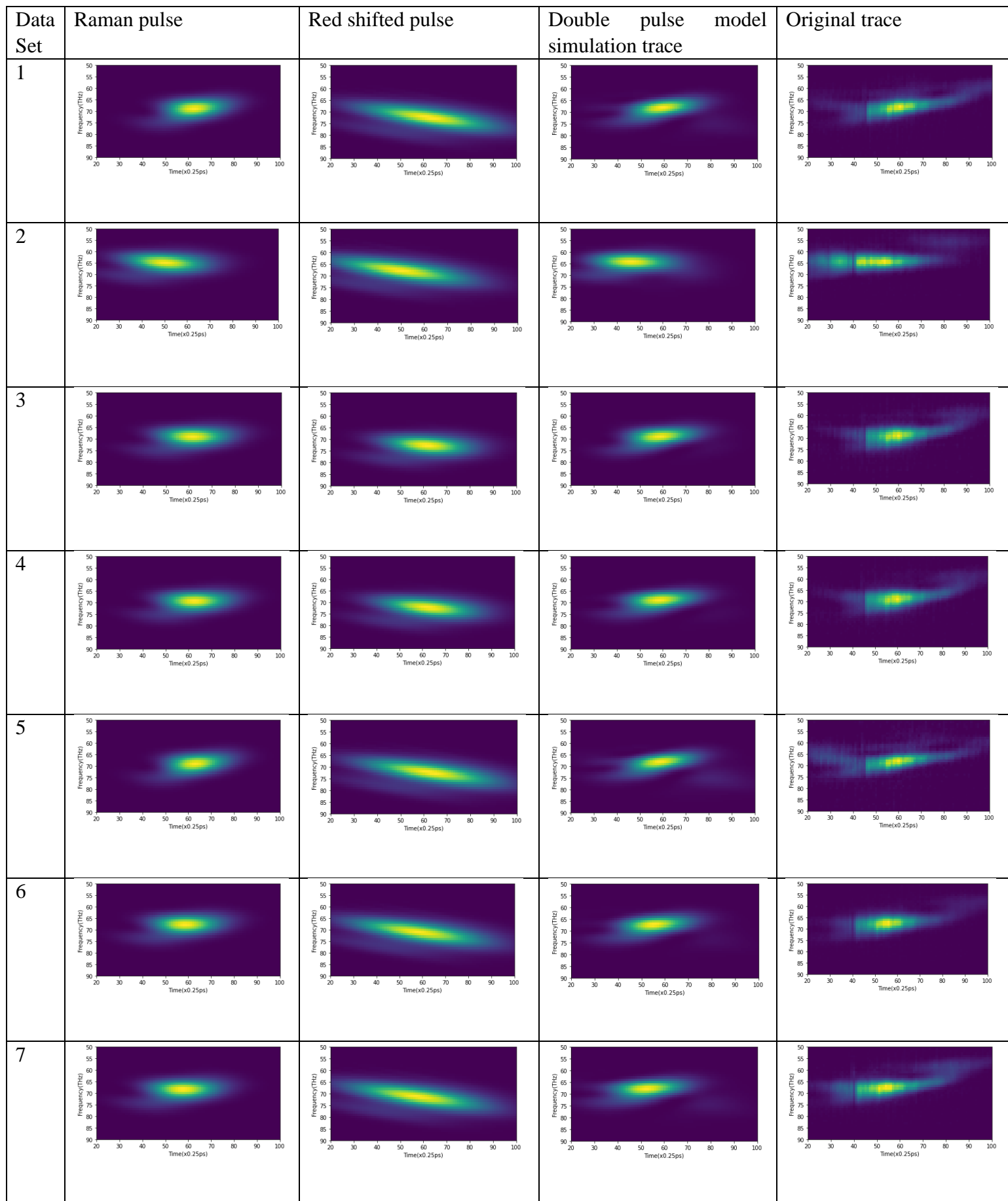
In the latest simulation, the data showed the same pattern and trend as the theory. From Table 3.11, the errors are similar to the error from the FROG program. Both the energy jitter, which controls the amplitude of generalized Rabi frequency, and the time delay, which controls the frequency separation, fit the predictions.

From theory and experimental setting, the average amplitude of the generalized Rabi frequency (represented by ff in the Table 11) for case A, B, C, D and E should be different because the instantaneous frequency separation increases with the red and blue shifting. From the Table 3.11, the average value of ff for A, B, C, D and E are $0.92*10^{-4}$, $1.7*10^{-4}$, $2.56*10^{-4}$, $2.3*10^{-4}$ and $0.67*10^{-4}$ respectively.

For the time jitter, the tpp*dd is used to represent it. The average values of time jitter for case A, B, C, D and E are expected to be -666fs, -333fs, 0fs, 333fs and 666fs. The average simulated result for case A, B, C, D and E are -559fs, -352fs, 44fs, 284fs, 514fs respectively. Hence, the results showed the same trend as the two-photon Stark shift and Rabi frequency theory.

Meanwhile, the two-photon Stark shift and Rabi frequency theory can explain the absence of the blue shifted spectra. From Figure 2.4 (b), the blue shifted pulses require the pump pulses to start at the E^+ level on the ground state. This is a very strict condition because the particle density at E^+ level on the ground state is very low. Consequently, it is hard to observe the blue shifted spectra in MRG experiment.

On the other hand, from Table 3.11, the amplitude of generalized Rabi frequency for case A and E, is very low. Hence, I also tried to use linear chirp as the blue and red shifted pulse because I want to find out how the 4-wave mixing effect impacts the MRG process. Surprisingly, I can also get good match and reasonable simulation results for case A and E. The data, instantaneous frequency and simulated trace are shown in Table 3.12 to 3.16.

Data Set	Raman pulse	Red shifted pulse	Double pulse model simulation trace	Original trace
1				
2				
3				
4				
5				
6				
7				

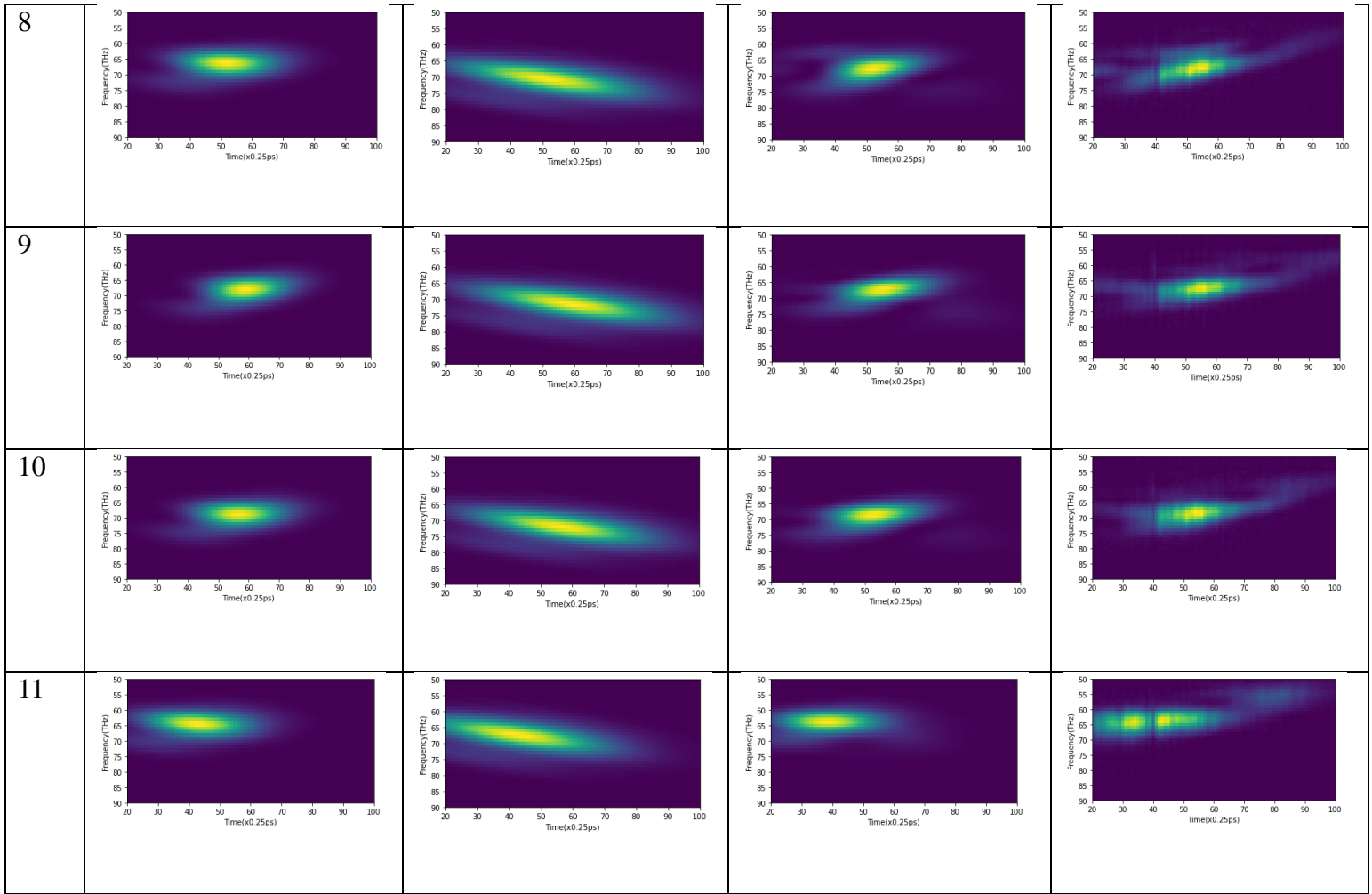|			
8				
9				
10				
11				

Table 3.12. Simulated and original trace for 11 data set of case A (4-wave mixing).

Unit for x-axis: 46.77109 fs/pixel. Unit for y-axis: 0.1670369 THz/pixel.

Data Set	Raman pulse	Red shifted pulse	Double pulse model simulation trace	Original trace
1				
2				
3				
4				
5				
6				
7				

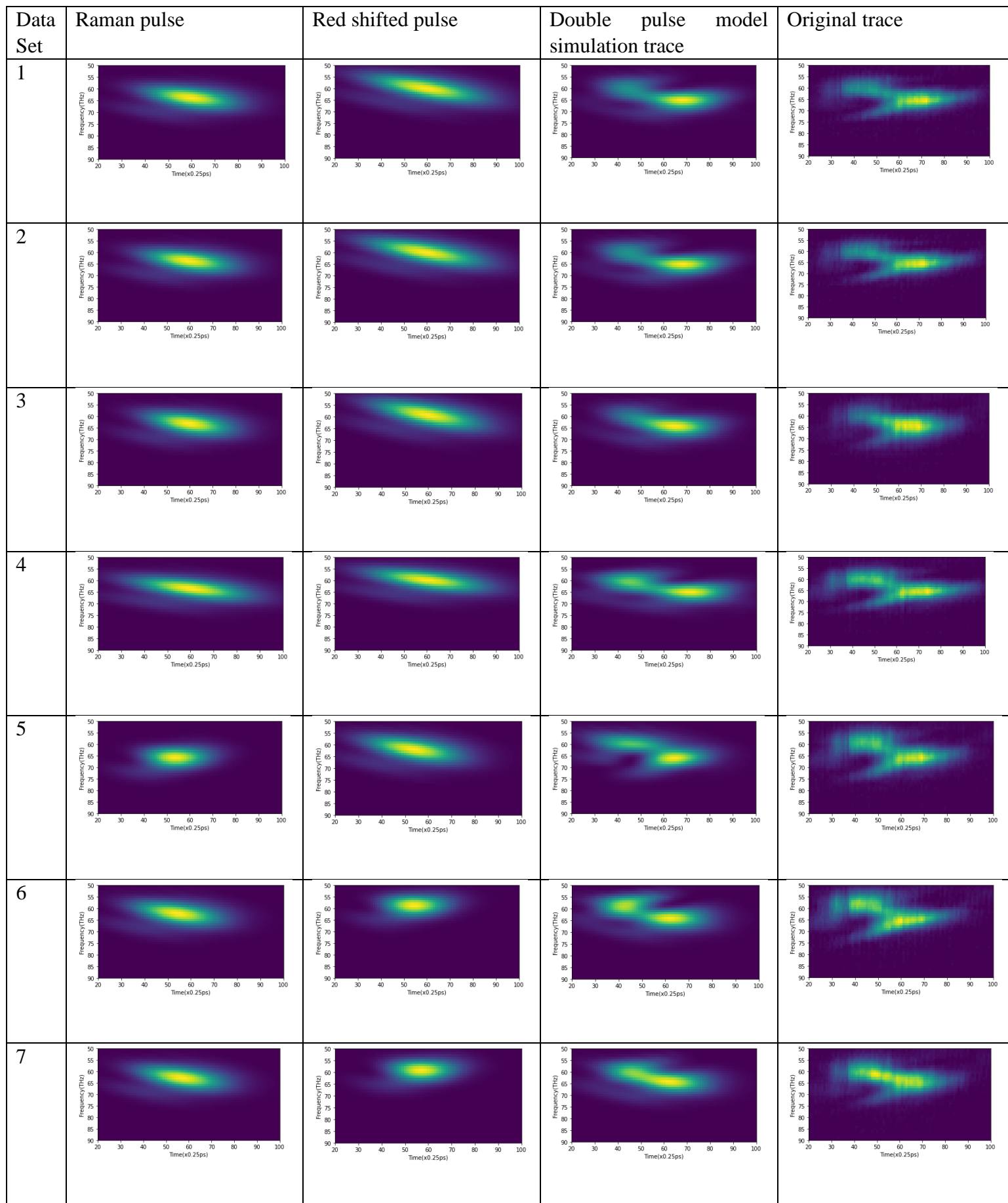|				
8				
9				
10				
11				

Table 3.13. Simulated and original trace for 11 data set of case E (4-wave mixing).

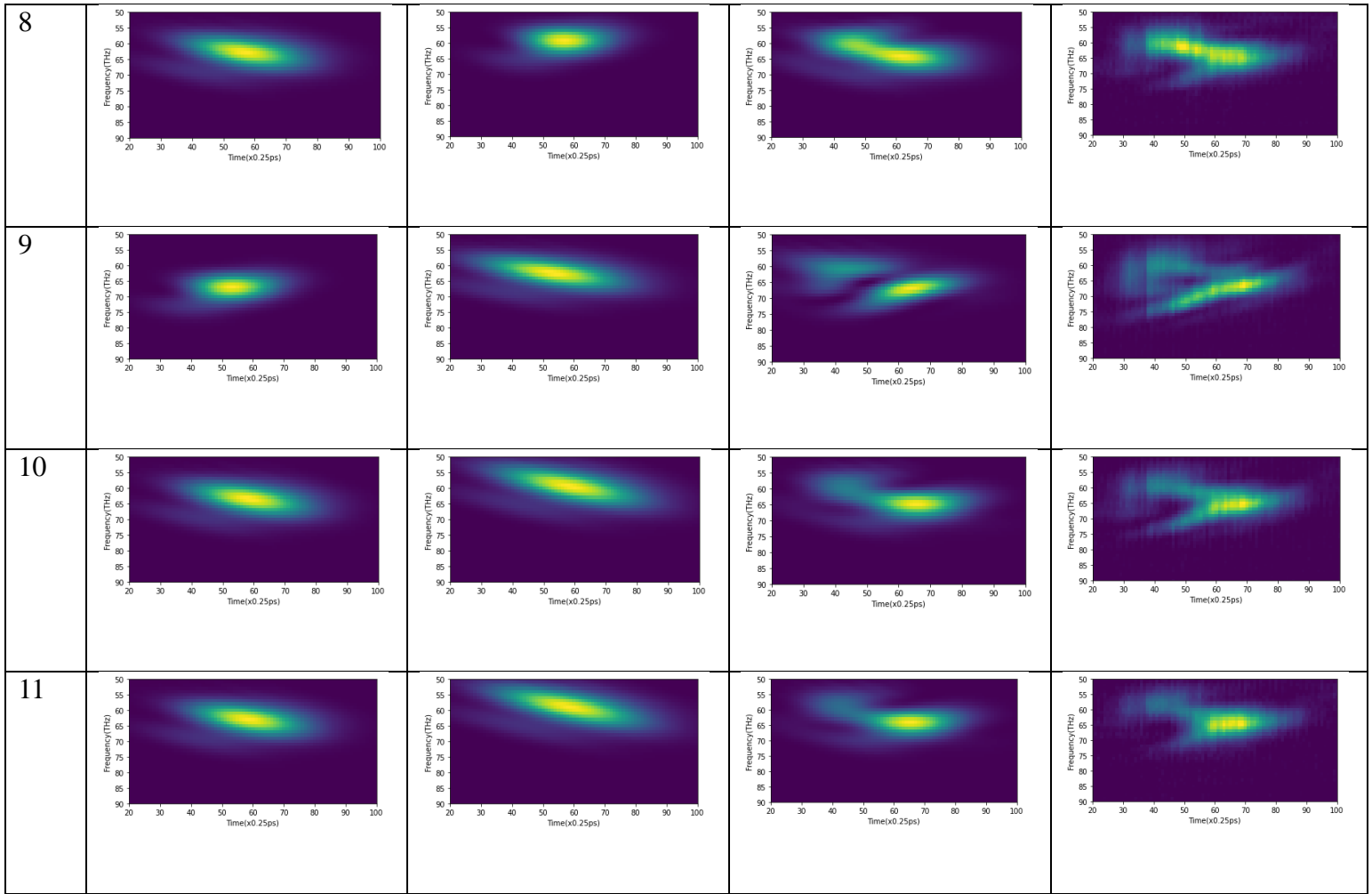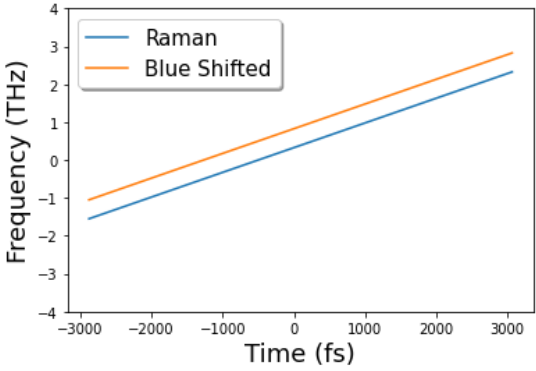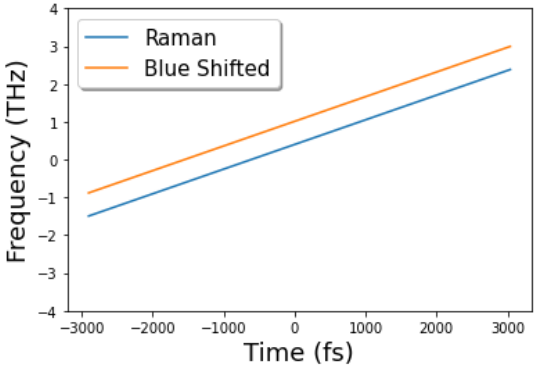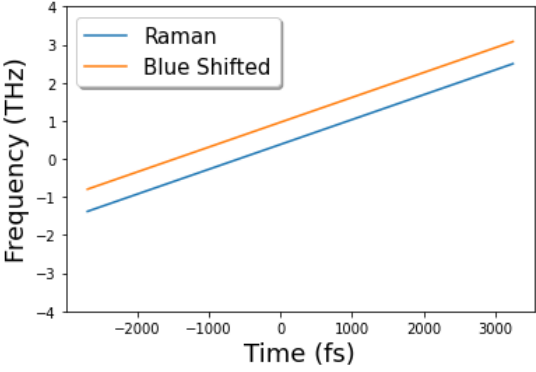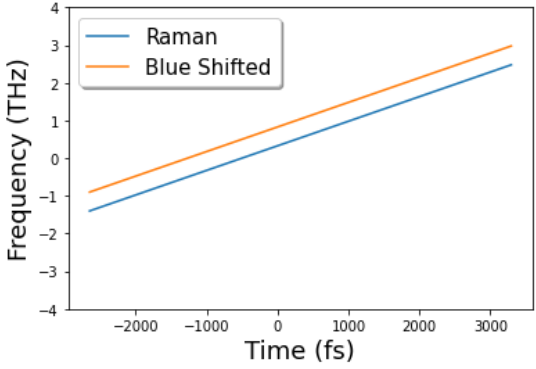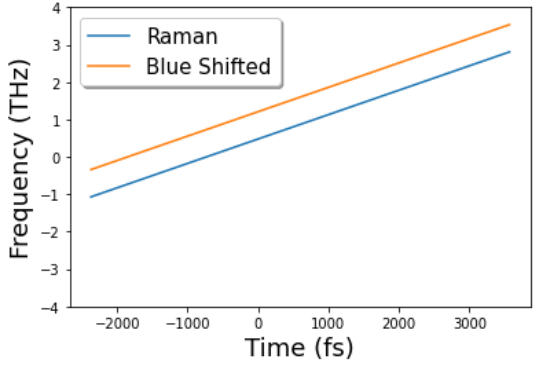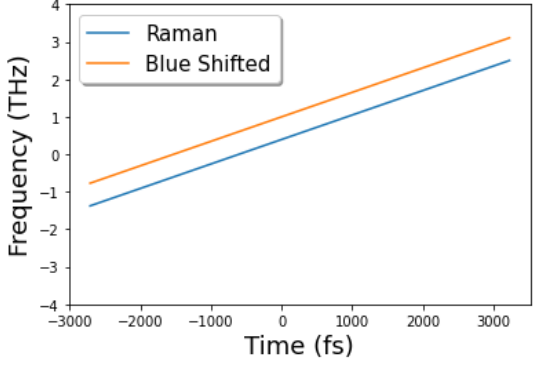Unit for x-axis: 46.77109 fs/pixel. Unit for y-axis: 0.1670369 THz/pixel.

Data Set	Parameter	Number	Instantaneous frequency (Blue: Raman pulse. Orange: Blue shifted pulse)
1	Error	0.078	
	T1(fs)	627	
	T2(fs)	2000	
	TT0(fs)	0	
	tpp(fs)*dd	-640	
	A	3.35	
	a2	0.0000041	
	f0	0.00087	
	ph0	-2.48	
	ff	0	
	tt(fs)	2876	
Data Set	Parameter	Average number	Instantaneous frequency (Blue: Raman pulse. Orange: Blue shifted pulse)
2	Error	0.12	
	T1(fs)	1106	
	T2(fs)	2000	
	TT0(fs)	0	
	tpp(fs)*dd	-500	
	A	5.25	
	a2	0.0000041	
	f0	0.00023	
	ph0	-3.96	
	ff	0	
	tt(fs)	2303	
Data Set	Parameter	Average number	Instantaneous frequency (Blue: Raman pulse. Orange: Blue shifted pulse)
3	Error	0.059	
	T1(fs)	833	
	T2(fs)	1167	
	TT0(fs)	0	
	tpp(fs)*dd	-500	
	A	3.15	
	a2	0.0000041	
	f0	0.00092	
	ph0	-2.05	
	ff	0	
	tt(fs)	2830	

Data Set	Parameter	Average number	Instantaneous frequency (Blue: Raman pulse. Orange: Blue shifted pulse)
4	Error	0.055	
	T1(fs)	781	
	T2(fs)	1389	
	TT0(fs)	0	
	tpp(fs)*dd	-500	
	A	2.75	
	a2	0.0000041	
	f0	0.00097	
	ph0	-2.05	
	ff	0	
	tt(fs)	2876	
Data Set	Parameter	Average number	Instantaneous frequency (Blue: Raman pulse. Orange: Blue shifted pulse)
5	Error	0.12	
	T1(fs)	600	
	T2(fs)	2000	
	TT0(fs)	0	
	tpp(fs)*dd	-612	
	A	2.65	
	a2	0.0000041	
	f0	0.00089	
	ph0	-2.49	
	ff	0	
	tt(fs)	2901	
Data Set	Parameter	Average number	Instantaneous frequency (Blue: Raman pulse. Orange: Blue shifted pulse)
6	Error	0.043	
	T1(fs)	796	
	T2(fs)	2000	
	TT0(fs)	0	
	tpp(fs)*dd	-582	
	A	3.65	
	a2	0.0000041	
	f0	0.00069	
	ph0	-2.64	
	ff	0	
	tt(fs)	2694	

Data Set	Parameter	Average number	Instantaneous frequency (Blue: Raman pulse. Orange: Blue shifted pulse)
7	Error	0.089	
	T1(fs)	804	
	T2(fs)	2000	
	TT0(fs)	0	
	tpp(fs)*dd	-500	
	A	2.65	
	a2	0.0000041	
	f0	0.00081	
	ph0	-2.93	
	ff	0	
	tt(fs)	2646	
Data Set	Parameter	Average number	Instantaneous frequency (Blue: Raman pulse. Orange: Blue shifted pulse)
8	Error	0.071	
	T1(fs)	898	
	T2(fs)	2000	
	TT0(fs)	0	
	tpp(fs)*dd	-730	
	A	2.55	
	a2	0.0000041	
	f0	0.00048	
	ph0	-2.62	
	ff	0	
	tt(fs)	2371	
Data Set	Parameter	Average number	Instantaneous frequency (Blue: Raman pulse. Orange: Blue shifted pulse)
9	Error	0.067	
	T1(fs)	641	
	T2(fs)	2000	
	TT0(fs)	0	
	tpp(fs)*dd	-604	
	A	3.15	
	a2	0.0000041	
	f0	0.00074	
	ph0	-3.08	
	ff	0	
	tt(fs)	2712	
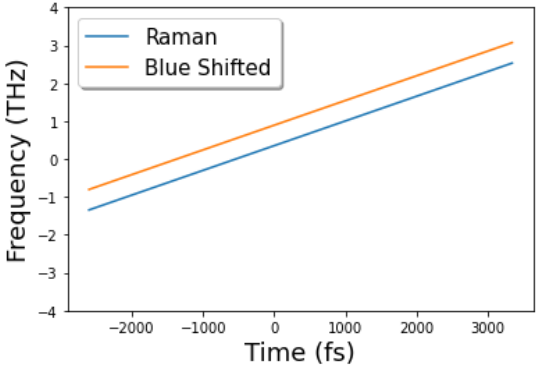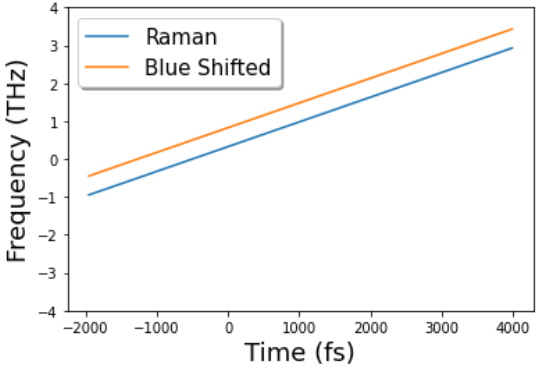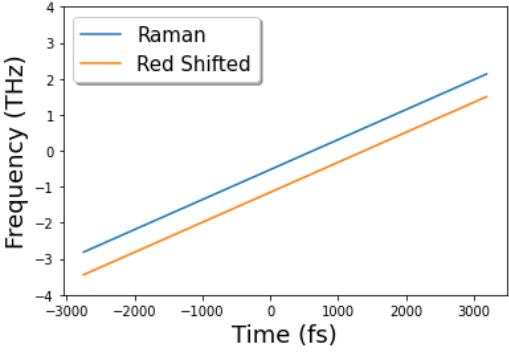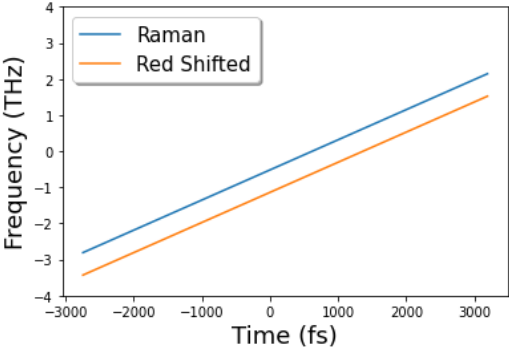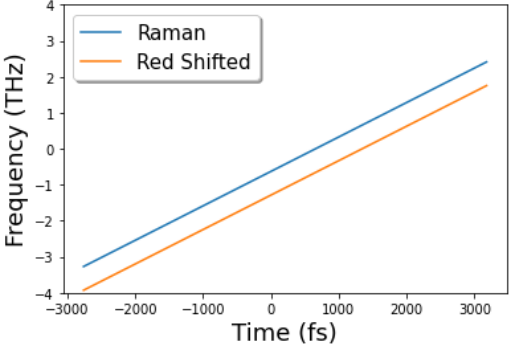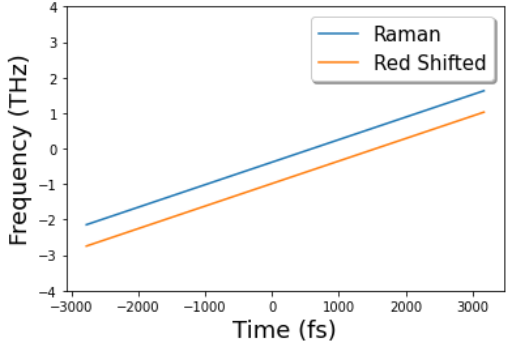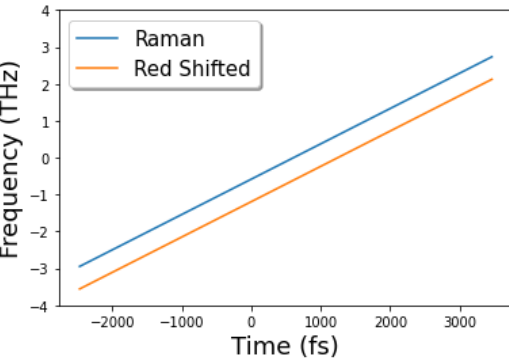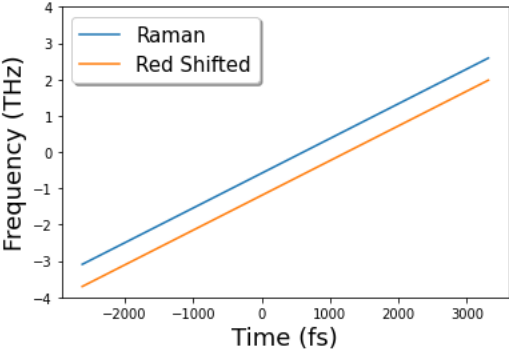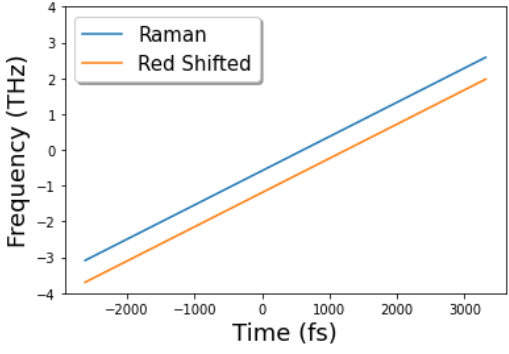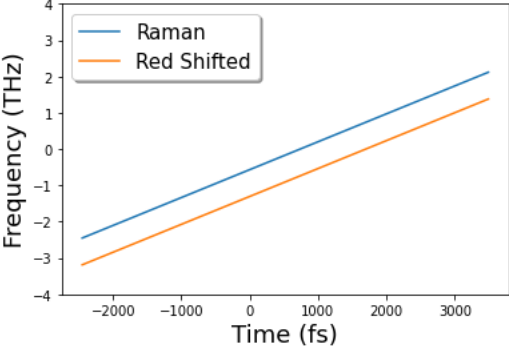
Data Set	Parameter	Average number	Instantaneous frequency (Blue: Raman pulse. Orange: Blue shifted pulse)
10	Error	0.049	
	T1(fs)	798	
	T2(fs)	1927	
	TT0(fs)	0	
	tpp(fs)*dd	-540	
	A	2.75	
	a2	0.0000041	
	f0	0.00088	
	ph0	-2.72	
	ff	0	
	tt(fs)	2600	
Data Set	Parameter	Average number	Instantaneous frequency (Blue: Raman pulse. Orange: Blue shifted pulse)
11	Error	0.12	
	T1(fs)	600	
	T2(fs)	2000	
	TT0(fs)	0	
	tpp(fs)*dd	-500	
	A	2.45	
	a2	0.0000041	
	f0	-0.00095	
	ph0	-2.41	
	ff	0	
	tt(fs)	2926	

Table 3.14. The data and instantaneous frequency of case A (4-wave mixing). Left - Simulation results for 11 data sets of case A (666fs blue shifted pulses). Right - The instantaneous frequency of the Raman pulse and blue shifted pulse.

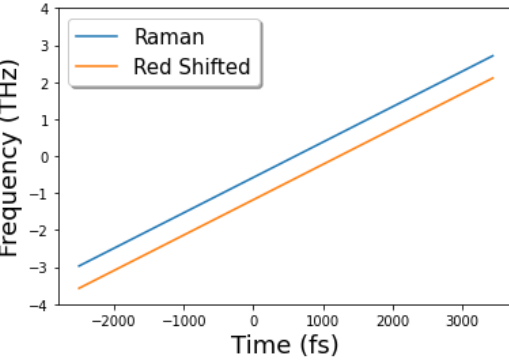| Data Set	Parameter	Number	Instantaneous frequency (Blue: Raman pulse. Orange: Blue shifted pulse)
1	Error	0.039	
	T1(fs)	1264	
	T2(fs)	1693	
	TT0(fs)	0	
	tpp(fs)*dd	630	
	A	3.1	
	a2	0.00000523	
	f0	0.00006	
	ph0	4.29	
	ff	0	
	tt(fs)	2750	
Data Set	Parameter	Average number	Instantaneous frequency (Blue: Raman pulse. Orange: Blue shifted pulse)
2	Error	0.039	
	T1(fs)	1254	
	T2(fs)	1700	
	TT0(fs)	0	
	tpp(fs)*dd	622	
	A	3.1	
	a2	0.00000524	
	f0	0.00005	
	ph0	4.27	
	ff	0	
	tt(fs)	2746	
Data Set	Parameter	Average number	Instantaneous frequency (Blue: Raman pulse. Orange: Blue shifted pulse)
3	Error	0.025	
	T1(fs)	1161	
	T2(fs)	1528	
	TT0(fs)	0	
	tpp(fs)*dd	658	
	A	5.8	
	a2	0.00000601	
	f0	-0.00004	
	ph0	4.53	
	ff	0	
	tt(fs)	2761	

Data Set	Parameter	Average number	Instantaneous frequency (Blue: Raman pulse. Orange: Blue shifted pulse)
4	Error	0.071	
	T1(fs)	1700	
	T2(fs)	1700	
	TT0(fs)	0	
	tpp(fs)*dd	600	
	A	3.3	
	a2	0.000004	
	f0	0.00001	
	ph0	3.82	
	ff	0	
	tt(fs)	2773	
Data Set	Parameter	Average number	Instantaneous frequency (Blue: Raman pulse. Orange: Blue shifted pulse)
5	Error	0.05	
	T1(fs)	700	
	T2(fs)	1313	
	TT0(fs)	0	
	tpp(fs)*dd	610	
	A	0.5	
	a2	0.00000601	
	f0	0.00037	
	ph0	5.47	
	ff	0	
	tt(fs)	2472	
Data Set	Parameter	Average number	Instantaneous frequency (Blue: Raman pulse. Orange: Blue shifted pulse)
6	Error	0.096	
	T1(fs)	1180	
	T2(fs)	700	
	TT0(fs)	0	
	tpp(fs)*dd	600	
	A	2.1	
	a2	0.00000601	
	f0	-0.0002	
	ph0	4.67	
	ff	0	
	tt(fs)	2504	

Data Set	Parameter	Average number	Instantaneous frequency (Blue: Raman pulse. Orange: Blue shifted pulse)
7	Error	0.027	
	T1(fs)	1180	
	T2(fs)	700	
	TT0(fs)	0	
	tpp(fs)*dd	610	
	A	3.8	
	a2	0.00000601	
	f0	-0.00011	
	ph0	4.15	
	ff	0	
	tt(fs)	2623	

Data Set	Parameter	Average number	Instantaneous frequency (Blue: Raman pulse. Orange: Blue shifted pulse)
8	Error	0.028	
	T1(fs)	1196	
	T2(fs)	700	
	TT0(fs)	0	
	tpp(fs)*dd	610	
	A	3.9	
	a2	0.000006	
	f0	-0.00011	
	ph0	4.13	
	ff	0	
	tt(fs)	2623	

Data Set	Parameter	Average number	Instantaneous frequency (Blue: Raman pulse. Orange: Blue shifted pulse)
9	Error	0.12	
	T1(fs)	700	
	T2(fs)	1529	
	TT0(fs)	0	
	tpp(fs)*dd	738	
	A	1	
	a2	0.00000483	
	f0	0.00057	
	ph0	5.77	
	ff	0	
	tt(fs)	2449	
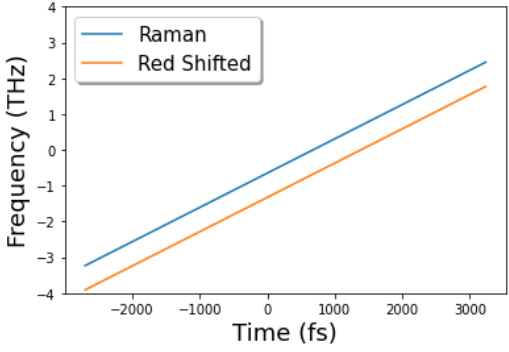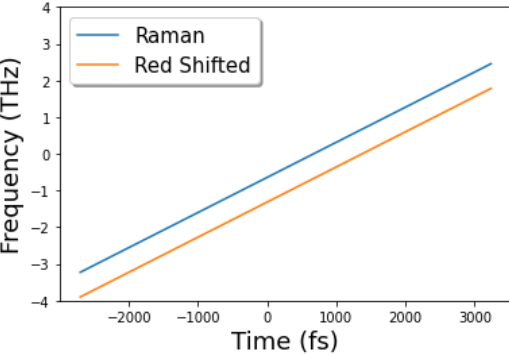
Data Set	Parameter	Average number	Instantaneous frequency (Blue: Raman pulse. Orange: Blue shifted pulse)
10	Error	0.076	
	T1(fs)	1221	
	T2(fs)	1558	
	TT0(fs)	0	
	tpp(fs)*dd	680	
	A	3.3	
	a2	0.000006	
	f0	0.00001	
	ph0	4.79	
	ff	0	
	tt(fs)	2701	

Data Set	Parameter	Average number	Instantaneous frequency (Blue: Raman pulse. Orange: Blue shifted pulse)
11	Error	0.042	
	T1(fs)	1186	
	T2(fs)	1604	
	TT0(fs)	0	
	tpp(fs)*dd	672	
	A	3.2	
	a2	0.000006	
	f0	-0.00008	
	ph0	4.92	
	ff	0	
	tt(fs)	2703	

Table 3.15. The data and instantaneous frequency of case E (4-wave mixing). Left - Simulation results for 11 data sets of case E (333 fs blue shifted pulses). Right - The instantaneous frequency of the Raman pulse and blue shifted pulse.

Case	A	B	C	D	E
Error	0.079	0.072	0.101	0.092	0.055
T1(fs)	771	1403	1142	1100	1158
T2(fs)	1862	795	897	790	1338
TT0(fs)	0	890	467	708	0
tpp*dd	-564	-352	44	284	639
A	3.12	0.51	1.09	0.79	3.0
a2	$4.1*10^{-6}$	$4.0*10^{-6}$	$5.07*10^{-6}$	$6.24*10^{-6}$	$5.57*10^{-6}$
f0	$5.9*10^{-4}$	$3.8*10^{-4}$	$4.7*10^{-4}$	$6.16*10^{-4}$	$4.62*10^{-5}$
ph0	-2.67	0.96	-2	3.78	4.6
ff	0	$1.7*10^{-4}$	$2.56*10^{-4}$	$2.3*10^{-4}$	0
tt(fs)	2703	2194	2221	2674	2645

Table 3.16. The average data of 11 simulated traces from the double pulse model simulation program for five cases (with case A and E as 4-wave mixing).

From the data and results, for case A and E, the gaussian dips in the middle are so small that could be ignored. That is because in those cases, the overlapped part of pump and Stokes are smaller, resulting in smaller amplitude of two-photon Stark shift and Rabi frequency. Consequently, the 4-wave mixing effect is much more dominant. In conclusion, the case A and E, the blue or red shift is mainly from the 4-wave mixing and for the case B, C and D, the red or blue shift is from the two-photon Stark

shift and Rabi frequency.

3.2 Simulation Results with Different Time Delay

After 2 years of study and simulation, I decided to focus on the red shifted cases, and the cases with different energy. Meanwhile, the double pulse model simulation model is also improved. The program is shown below.

```
def FROGs(params):

    [T1,T2,A,f0,tau,t_j,a2,ph0,en_f] = params

    E_S = gaussian_pulse(TT1,0,1.0,0,tau-(1000*td_f/3.0+t_j))#generate
Gaussian pulse E-field

    E_p = gaussian_pulse(TT2,0,1.0,0,tau)

    i1 = E_p**2

    i2 = E_p**2 + E_S**2

    i3 = i1*E_S


    DELTA_0     =     2*np.pi*(a22-a11)*A0*en_f*i2/(c0*h/(2*np.pi))/(10**12)-
0.33*(td_f+3*t_j/1000)/1000*2*np.pi

    Omega = 2*np.pi*a12*A0*en_f*i3/(c0*h/(2*np.pi))/(10**12)

    e_diff = np.sqrt(DELTA_0**2+Omega**2)
```

```
phase1 = a2*(t-tau)                    #zero phase at pulse peak

phase1 = integral(-phase1)

phase1 = phase1-phase1[63]

phase2 = a2*(t-tau)-e_diff/(2*np.pi)

phase2 = integral(-phase2)

phase2 = phase2-phase2[63]+ph0



E1 = gaussian_pulse(T1,f0,A,phase1,tau)     #generate Gaussian pulse E-field

E2 = gaussian_pulse(T2,f0,1.0,phase2,tau)

E = E1+E2



FROG = FROG_generator(e,E,TD)

return FROG
```

In the program, there are 9 different parameters to control the simulation of the total Raman pulse. They are T1 (Pulse duration of the Raman pulse (E_1)), T2 (Pulse duration of the red shifted pulse (E_2)), f0 (Center frequency), tau (Time delay), t_j (Time jitter), a2 (The chirp rate of instantaneous frequency), ph0 (Π phase shift) and en_f (Amplitude coefficient of Rabi frequency). The td_f is the parameter, which controls the frequency separation of the instantaneous frequency of E_1 and E_2 for different cases.

73

The DELTA_0 is the total detuning, $\Delta(t)$. The Omega is the Rabi frequency, Ω. The e_diff is the total Rabi frequency, which is shown in Equation (13). The phase of Raman part is only a second order phase, which is the integral of a linear instantaneous frequency. Meanwhile, the phase of the red shifted part consists of a second order phase, a pi phase shift and the integral of generalized Rabi frequency. The E_1 and E_2 are Raman pulse and red shifted pulse. E is the total Raman pulse.

In this part, the MRG procedure with varied instantaneous frequencies is explored, achieved by adjusting the time delays between the pump and Stokes pulses. They are case C, D and E with three different time delays: 0 fs, 333 fs, and 666 fs respectively. Each case has 11 original traces. Figure 3.2 and Table 3.17 below display the simulation results and experimental data for three different cases.
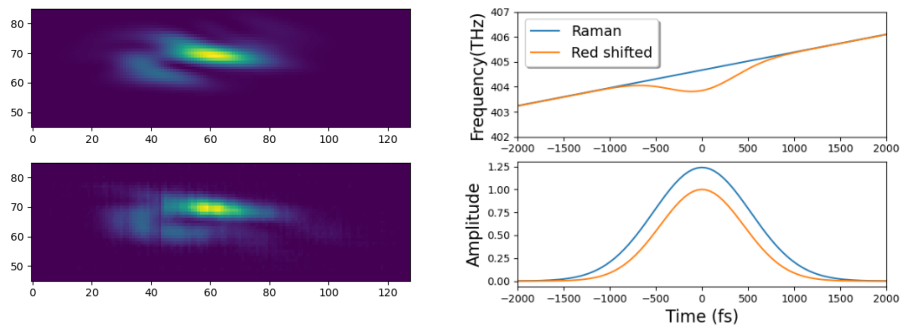
(a) Case C
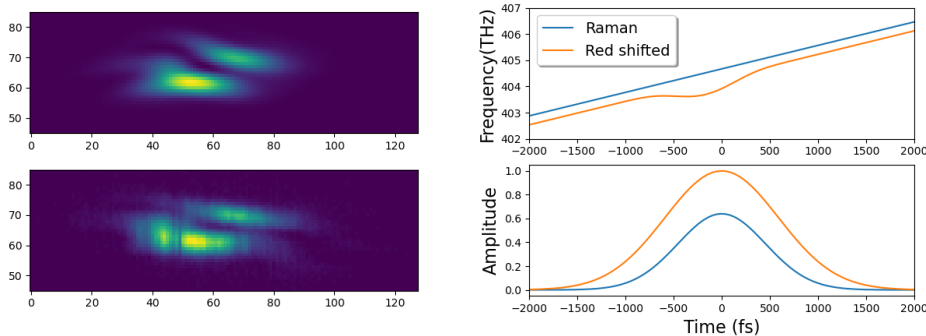
(b) Case D
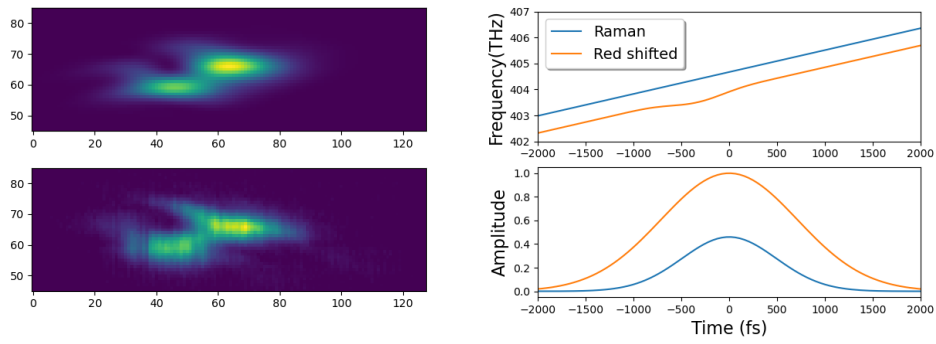
(c) Case E

Figure 3.2. Simulation results with different time delay by new program. Left: up-The instantaneous frequency of the Raman pulse and red shifted pulse with different energy, down-the amplitudes; Right: up-Simulation, down-experimental data. Unit for x-axis: 46.77109 fs/pixel. Unit for y-axis: 0.1670369 THz/pixel. (a) Case C: Timed pulses; (b) Case D: 333 fs red shifted pulse; (c) Case E: 666 fs red shifted pulse.

Case	C	D	E
Error	0.123	0.094	0.057
T1 (fs)	968.8	793.2	809.6
T2 (fs)	883.5	1052.8	1383.9
A	1.145	0.677	0.406
f0	0.00071	0.000712	0.000525
tau (fs)	2283.4	2665	2592.2
t_j (fs)	-0.364	9.34	12.1
a2	4.24E-06	5.66E-06	5.25E-06
ph0	3.75	3.88	4.62
en_f	2.22	2.47	2.5
td_f = 0	0	1	2

Table 3.17. The average data of 11 simulated traces from the double pulse model simulation program for different cases with different time detuning at around 0 fs, 333 fs and 666 fs. The energy is at around 2.2 mJ. T1 (Pulse duration of the Raman pulse (E_1)), T2 (Pulse duration of the red shifted pulse (E_2)), A (Amplitude ratio between Raman pulse and Red shifted pulse), f0 (Center frequency), f0 (Center frequency), tau (Time delay), t_j (Time jitter), a2 (The chirp rate of instantaneous frequency), ph0 (Π phase shift) and en_f (Amplitude coefficient of Rabi frequency). The td_f is the parameter, which controls the frequency separation of the instantaneous frequency of E_1 and E_2 for different cases.

In Figure 3.2, the simulated trace looks very similar to the original trace from experiments. The instantaneous frequency of the Raman pulse is linear chirp, and the instantaneous frequency of the red shifted pulse is linear chirp with a gaussian dip in the middle. It is clear that the dip in the middle of instantaneous frequency becomes smaller when the time delay becomes bigger. In Figure 3.2 (a), The instantaneous frequency of Raman and red shifted pulse are overlapped at the edges. This is because the pulses are resonant with the Raman transition which make the total detuning at zero on the edge. On the other hand, the reason why the instantaneous frequency becomes larger at the center is that the Stark shift and Rabi frequency were maximized when the two pump pulses overlapped with each other. For Figure 3.2 (b) and (c), when the time delay becomes larger, the Raman scattering moved away from resonance, causing the red shifted pulse to grow and take the lead. The time delay also results in the constant detuning on the instantaneous frequency of red shifted pulses.

From Table 3.17, the average error for case D and E are lower than 0.1 which is better than the results from FROG. For case C, the average error is 0.123, which is at the

same level as the results from FROG. The instantaneous frequency separation between Raman pulse and red shifted pulse is equal to td_f*333+t_j (fs). The average instantaneous frequency separations for C, D and E cases are at -0.364 fs, 332.34 fs and 678.1 fs. The average chirp rates of the Raman and red shifted pulses are similar to that of the pump pulse.

The average pulse duration of E_1 is around 800 fs, whereas the average pulse duration of E_2 goes up from 883.8 fs for case C, 1052.8 fs for case D to 1383.9 fs for case E. At the same time, the parameter A, amplitude ratio between Raman pulse and Red shifted pulse, decreases from 1.145 for case C, 0.677 for case D to 0.406 for case E. From this trend of T2 and C, the red shifted pulse becomes stronger when the time delay becomes larger. This observation is attributed to the time mismatch between the pump and the overlapped region of the pump and Stokes pulses.

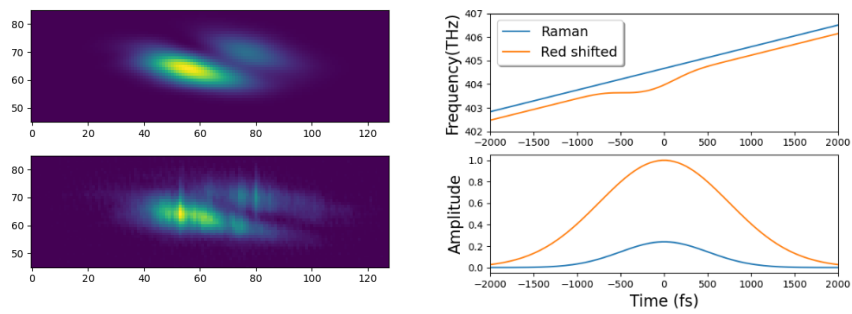## 3.3 Simulation Results with Different Energy

In the next stage, the simulation results and the experimental results for the three different energies of 1.2 mJ, 1.7 mJ and 2.2 mJ at the pump pulse delay of 333fs are compared. These results are shown in Figure 3.3 and the modelled time varying frequency shift increases in magnitude with increasing pulse energy.

For each set of 3 measurements, the red shifted pulse with different pulse energies is compared. The pulse duration for the pumps is given by the FROG measurements of the pumps. The beam area was given by the diameter of the hollow fiber, which was 150μm and 30% of the light was transmitted through fiber. The fiber emits white light along most of the fiber, indicating loss of power with over the length [7]. The energy is measured before the hollow fiber and the experiments are performed at three
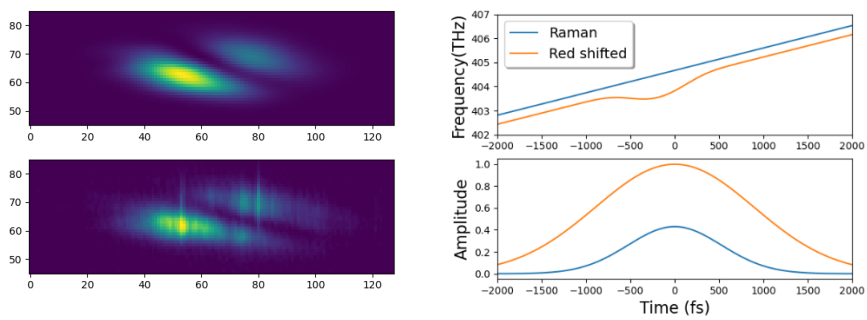
77

average energies of 1.2 mJ, 1.7 mJ and 2.2 mJ. In the model, the average energy

before the fiber is represented by the variable coefficient en_f.
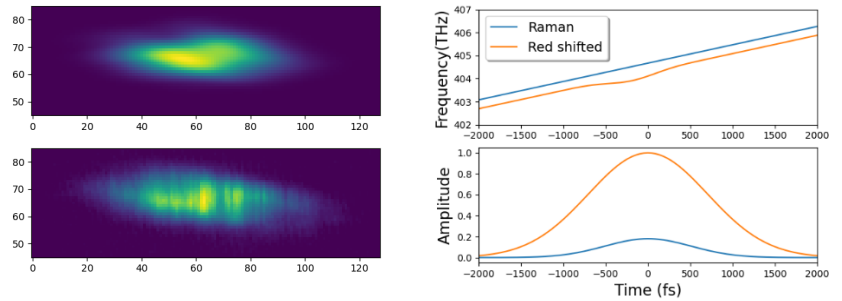
(a)

(b)

(c)

Figure 3.3. Simulation results with different intensity delay by new program. Left: up-

The instantaneous frequency of the Raman pulse and red shifted pulse with different

energy, down-the amplitudes; Right: up-Simulation, down-experimental data. Unit for x-axis: 46.77109 fs/pixel. Unit for y-axis: 0.1670369 THz/pixel. (a) 1.2 mJ. (b) 1.7 mJ. (c) 2.2 mJ.

Case	1.2mJ	1.7mJ	2.2mJ
Error	0.0869	0.058	0.0887
T1 (fs)	900	833.9	897
T2 (fs)	1420.1	1180.8	1292.9
A	0.155	0.217	0.767
f0	0.00106	0.00088	0.00119
tau (fs)	2953.4	2988.7	2683.8
t_j (fs)	58.5	21.47	39.8
a2	5.2E-06	5.38E-06	5.52E-06
ph0	2.1	1.51	4.057
en_f	1.5	2.04	2.88
td_f = 0	1	1	1

Table 3.18. The average data of 3 simulated traces from the double pulse model simulation program for different cases with energy at 1.2 mJ, 1.7 mJ and 2.2 mJ. The time detuning is at around 333 fs. T1 (Pulse duration of the Raman pulse (E_1)), T2 (Pulse duration of the red shifted pulse (E_2)), A (Amplitude ratio between Raman pulse and Red shifted pulse), f0 (Center frequency), tau (Time delay), t_j (Time jitter), a2 (The chirp rate of instantaneous frequency), ph0 (Π phase shift) and en_f (Amplitude coefficient of Rabi frequency). The td_f is the parameter, which controls the frequency separation of the instantaneous frequency of E_1 and E_2 for different cases.

From Table 3.18, the average error for all three cases is lower than 0.1 which is better than the results from FROG. The pulse duration for E_1 and E_2 are around 850 fs and

1300 fs which fits expectation. The instantaneous frequency separation between Raman pulse and red shifted pulse is equal to td_f*333+t_j (fs). The instantaneous frequency separations for three energy cases are similar. The chirp rates of the Raman and red shifted pulses are similar to that of the pump pulse, which at about 5.0E-06.

In Figure 3.3, the simulated trace looks very similar to the original trace from experiments. The dip in the middle of linear instantaneous frequency of red shifted pulse are caused by Rabi frequency. The amplitude coefficient of Rabi frequency en_f is related to the middle dip of linear instantaneous frequency of red shifted pulse. The higher the en_f is, the deeper the dip is. From the Equation (5) and (7), the amplitude of the Rabi frequency is energy dependent, which means that the Rabi frequency becomes bigger when the energy increases. Meanwhile, from Table 1, the en_f for different energy cases with 1.2 mJ, 1.7 mJ and 2.2 mJ are at 1.5, 2.01 and 2.88 respectively, which would agree well with a final transmission of 30% of the total energy. This shows the same trend as the theory about the Rabi frequency.

Chapter 4

Conclusion

In this paper, I have compared experimental FROG spectrograms of the first anti-Stokes order of MRG spectrum to a double pulse model simulation spectrogram derived from the two-photon Rabi frequency and Stark shift of the resonant Raman process. From the figures and tables above, the result does fit the expectation and theory. The errors between double pulse model simulation and the experiment results are around or lower than 0.1, which is at the same level as the results from FROG. It helps researchers gain more understanding about the structure of the Raman pulse and red shifted pulse. The Rabi frequency is intensity dependent, and the intensity of the red shifted pulse will become stronger when the time delay becomes larger. These data and analysis prove that the generation of red shifted spectra in MRG experiment is from the two-photon Stark shift and Rabi frequency.

In the next stage, more experiments with different time delay at 1000 fs, 1333 fs and 1666 fs should be done to study the intensity of red shifted pulse. Meanwhile, the researchers can also try to use more intense pump to do the MRG experiment and study the red shifted spectra. Those can help the researchers test the theory further.

In future research, the absence of the blue shifted spectra in MRG experiment is also an interesting topic to explore. From the simulation results for blue shifted cases, the 4-wave mixing effect is more dominant than the two-photon Stark shift and Rabi frequency. Hence, the 4-wave mixing process is one of the causes of absence of the blue shifted spectra. On the other hand, from the two-photon Stark shift and Rabi frequency theory, the blue shifted pulses require the pump pulses to start at the E^+

level on the ground state. The particle density at E^+ level on the ground state is very low, so it is hard to observe the blue shifted spectra in MRG experiments.

Furthermore, the double pulse model simulation can be improved by Artificial Intelligence and machine learning technologies. This will help the researchers obtain the data and simulation results in a faster and more convenient way. With the help of more efficient tools, the researchers will be able to gain a better understanding of the MRG experiment and process.

References

[1] Imasaka, T., Kawasaki, S. & Ishibashi, N. Generation of more than 40 laser emission lines from the ultraviolet to the visible regions by two-color stimulated raman effect. Appl. Phys. B 49, 389–392 (1989).

[2] Strickland, D. (2014). Review of Multi-Frequency Raman Generation. *Chinese Journal of Physics*, *52*(1), 546-568.

[3] Cui, Z., Chaturvedi, M., Tian, B., Ackert, J., Turner, F. C., & Strickland, D. (2013). Spectral red-shifting of multi-frequency Raman orders. *Optics Communications*, *288*, 118-121.

[4] Trebino, R. (2000). *Frequency-Resolved Optical Gating: The Measurement of Ultrashort Laser Pulses: The Measurement of Ultrashort Laser Pulses*. Springer Science & Business Media.

[5] Xu, Z., Jin, Z., & Strickland, D. (2022, May). Double-pulse Model for the Study of Red-shifted Spectrum in Multi-frequency Raman Generation. In 2022 Photonics North (PN) (pp. 1-1). IEEE.

[6] Li, S., Li, Y., Yi, R., Liu, L., & Qu, J. (2020). Coherent anti-Stokes Raman scattering microscopy and its applications. Frontiers in Physics, 8, 598420.

[7] Xu, Z. (2021). Red-shifted Spectrum in Multi-frequency Raman Generation.

[8] Schmidt, R., Fitzek, H., Nachtnebel, M., Mayrhofer, C., Schroettner, H., & Zankel, A. (2019, April). The combination of electron microscopy, Raman microscopy and energy dispersive X-ray spectroscopy for the investigation of polymeric materials. In Macromolecular symposia (Vol. 384, No. 1, p. 1800237).

[9] Turner, F. C., Trottier, A., Strickland, D. & Losev, L. L. Transient multi-frequency Raman generation in SF6. Optics Communications 270, 419–423 (2007).

[10] Zhang, Z., Deslauriers, A. M., & Strickland, D. (2000). Dual-wavelength chirped-pulse amplification system. *Optics Letters*, *25*(8), 581-583.

[11] Xu, Z., Rahnama, A., & Strickland, D. (2018, June). Temporal and Spectral Measurement of Red-Shifted Spectrum in Multi-Frequency Raman Generation. In 2018 Photonics North (PN) (pp. 1-1). IEEE.

[12] Sali, E., Mendham, K. J., Tisch, J. W. G., Halfmann, T. & Marangos, J. P. High-order stimulated Raman scattering in a highly transient regime driven by a pair of ultrashort pulses. Opt Lett 29, 495–497 (2004).

[13] Wang, K., Zhi, M., Hua, X., Strohaber, J., & Sokolov, A. V. (2014). Coherent broadband light generation with a double-path configuration. *Applied Optics*, *53*(13), 2866-2869.

[14] Bahari, A., Zhdanova, A. A., Shutova, M., & Sokolov, A. V. (2020). Synthesis of ultrafast waveforms using coherent Raman sidebands. *Physical Review A*, *102*(1), 013520.

[15] Tsang, T., Krumbügel, M. A., DeLong, K. W., Fittinghoff, D. N., & Trebino, R. (1996). Frequency-resolved optical-gating measurements of ultrashort pulses using surface third-harmonic generation. *Optics letters*, *21*(17), 1381-1383.

[16] Yan, H. & Strickland, D. Effect of Two-Photon Stark Shift on the Multi-Frequency Raman Spectra. Applied Sciences 4, 390–401 (2014).

[17] Lehmberg, R. H., Wolford, M. F., Weaver, J. L., Kehne, D., Obenschain, S. P., Eimerl, D., & Palastro, J. P. (2020). Stimulated rotational Raman scattering of arbitrarily polarized broadband light. *Physical Review A*, *102*(6), 063530.

[18] Wu, H., Song, Y., Zeng, Y., Zhu, G., Yu, G., & Yang, Y. (2022). Femtosecond coherent anti-Stokes Raman spectroscopy study of vibrational dynamics of liquid

chloroform. *RSC advances*, *12*(42), 27596-27603.

[19] Hickman, A. P., Paisner, J. A., & Bischel, W. K. (1986). Theory of multiwave propagation and frequency conversion in a Raman medium. *Physical review A*, *33*(3), 1788.

[20] Moore, W. C., Kim, A., Thompson, R. J., & Dedic, C. E. (2022). High resolution coherent anti-Stokes Raman scattering to study supersonic combustion. In AIAA SCITECH 2022 Forum (p. 1527).

[21] Rickes, T., Yatsenko, L. P., Steuerwald, S., Halfmann, T., Shore, B. W., Vitanov, N. V., & Bergmann, K. (2000). Efficient adiabatic population transfer by two-photon excitation assisted by a laser-induced Stark shift. The Journal of Chemical Physics, 113(2), 534-546.